

INDUCED-GRAVITY GUT-SCALE HIGGS INFLATION IN SUPERGRAVITY

CONSTANTINOS PALLIS¹ AND QAISAR SHAFI²

¹*School of Electrical & Computer Engineering, Faculty of Engineering,
Aristotle University of Thessaloniki, GR-541 24 Thessaloniki, GREECE*
e-mail address: kpallis@gen.auth.gr

²*Bartol Research Institute, Department of Physics and Astronomy,
University of Delaware, Newark, DE 19716, USA*
e-mail address: shafi@bartol.udel.edu

ABSTRACT: Models of induced-gravity inflation are formulated within Supergravity employing as inflaton the Higgs field which leads to a spontaneous breaking of a $U(1)_{B-L}$ symmetry at $M_{\text{GUT}} = 2 \cdot 10^{16}$ GeV. We use a renormalizable superpotential, fixed by a $U(1)$ R symmetry, and Kähler potentials which exhibit a quadratic non-minimal coupling to gravity with or without an independent kinetic mixing in the inflaton sector. In both cases we find inflationary solutions of Starobinsky type whereas in the latter case, others (more marginal) which resemble those of linear inflation arise too. In all cases the inflaton mass is predicted to be of the order of 10^{13} GeV. Extending the superpotential of the model with suitable terms, we show how the MSSM μ parameter can be generated. Also, non-thermal leptogenesis can be successfully realized, provided that the gravitino is heavier than about 10 TeV.

PACs numbers: 98.80.Cq, 04.50.Kd, 12.60.Jv, 04.65.+e

Published in *Eur. Phys. J. C* **78**, no. 6, 523 (2018).

I. INTRODUCTION

The idea of *induced gravity* (IG), according to which the (reduced) Planck mass m_{P} is generated [1] via the *vacuum expectation value* (v.e.v) that a scalar field acquires at the end of a phase transition in the early universe, has recently attracted a fair amount of attention. This is because it may follow an inflationary stage driven by a Starobinsky-type potential [2] in *Supergravity* (SUGRA) [3–7] and in non-*Supersymmetric* (SUSY) [8–12] settings, which turns out to be nicely compatible with the observational data [13]. As a bonus, the resulting effective theories do not suffer from any problem with perturbative unitarity [3, 5, 11, 14, 15] in sharp contrast to some models of non-minimal inflation [16–19] where the inflaton after inflation assumes a v.e.v much smaller than m_{P} .

The simplest way to realize the idea of IG is to employ a double-well potential, $\lambda(\phi^2 - v^2)^2$, for the inflaton ϕ [1, 3–5, 8–11] – scale invariant realizations of this idea are proposed in Ref. [12]. If we adopt a non-minimal coupling to gravity [9, 10] of the type $f_{\mathcal{R}} = c_{\mathcal{R}}\phi^2$ and set $v = m_{\text{P}}/\sqrt{c_{\mathcal{R}}}$, then $\langle f_{\mathcal{R}} \rangle = m_{\text{P}}^2$, i.e., $f_{\mathcal{R}}$ reduces to m_{P}^2 at the vacuum generating, thereby, Einstein gravity at low energies. The implementation of inflation, on the other hand, which requires the emergence of a sufficiently flat branch of the potential at large field values constrains $c_{\mathcal{R}}$ to sufficiently large values and λ as a function of $c_{\mathcal{R}}$. An even more restrictive version of this scenario would be achieved if ϕ is involved in a Higgs sector which triggers a *Grand Unified Theory* (GUT) phase transition in the early Universe [7, 9]. The scale of a such transition is usually related to the (field dependent) mass of the lightest gauge boson and can be linked to some unification condition in *supersymmetric* (SUSY) – most notably – settings [19–23]. As a consequence, $c_{\mathcal{R}}$ can be uniquely determined by the theoretical requirements, giving rise to an economical, predictive and well-motivated set-up, thereby called *IG Higgs inflation* (IGHI). To our knowledge, the unification hypothesis has not been previously employed in constraining IGHl.

Since gauge coupling unification is elegantly achieved within the *minimal supersymmetric standard model* (MSSM), we need to formulate IGHl in the context of SUGRA. Namely, we employ a renormalizable superpotential, uniquely determined by a gauge and a $U(1)$ R symmetry, which realizes the Higgs mechanism in a SUSY framework. Actually, this is the same superpotential widely used for the models of F-term hybrid inflation [24–28]. Contrary to that case, though, where the inflaton typically is a gauge singlet and a pair of gauge non-singlets are stabilized at zero, here the inflaton is involved in the Higgs sector of the theory whereas the gauge singlet superfield is confined at the origin playing the role of a *stabilizer* – for a related scenario see Ref. [29]. For this reason we call it *Higgs inflation* (HI). As regards the Kähler potentials, K , we concentrate on semi-logarithmic ones which employ variable coefficients for the logarithmic part and include only quadratic terms of the various fields, taking advantage of the recently established [6] stabilization mechanisms of the accompanying non-inflaton fields.

More specifically, we distinguish two different classes of K 's, depending whether we introduce an independent kinetic mixing in the inflaton sector or not. In the latter case the non-minimal coupling to gravity reads $f_{\mathcal{R}} \sim c_{\mathcal{R}}\phi^2$ and imposing the IG and unification conditions allows us to fully determine $c_{\mathcal{R}}$. In the former case, apart from the non-minimal coupling to gravity expressed as $f_{\mathcal{R}} = c_+\phi^2$, the models exhibit a kinetic mixing of the form $f_K \simeq c_-f_{\mathcal{R}}$, where the constants c_- and c_+ can be interpreted as the coefficients of the principal shift-symmetric term (c_-) and its violation (c_+) in the K 's. Obviously these models are inspired by the kinetically modified non-minimal HI studied in Ref. [20–23]. The observables now depend on the ratio $r_{\pm} = c_+/c_-$ which can be found precisely enforcing the IG and unification conditions. As a consequence, for both classes of models more robust predictions can be here achieved than those presented in the original papers [19–23], where m_{P} is included in $f_{\mathcal{R}}$ from every beginning. Most notably, the level of the predicted primordial

gravitational waves is about an order of magnitude lower than the present upper bound [13, 33] and may be detectable in the next generation of experiments [34–37].

We exemplify our proposal employing as “GUT” gauge symmetry $G_{B-L} = G_{\text{SM}} \times U(1)_{B-L}$, where $G_{\text{SM}} = SU(3)_C \times SU(2)_L \times U(1)_Y$ is the gauge symmetry of the standard model, and B and L denote baryon and lepton number respectively – cf. Ref. [20, 22, 23, 27]. The embedding of IGHI within this particle model gives us the opportunity to connect inflation with low energy phenomenology. In fact, the absence of the gauge anomalies enforces the presence of three right-handed neutrinos N_i^c which, in turn, generate the tiny neutrino masses via the type I seesaw mechanism. Furthermore, the out-of-equilibrium decay of the N_i^c 's provides us with an explanation of the observed *baryon asymmetry of the universe* (BAU) [38] via *non-thermal leptogenesis* (nTL) [39] consistently with the gravitino (\tilde{G}) constraint [40–43] and the data [44, 45] on the neutrino oscillation parameters. Also, taking advantage of the adopted R symmetry, the parameter μ appearing in the mixing term between the two electroweak Higgs fields in the superpotential of MSSM is explained as in Refs. [3, 23, 25] via the v.e.v of the stabilizer field, provided that the relevant coupling constant is appropriately suppressed. The post-inflationary completion induces more constraints testing further the viability of our models.

The remaining text is organized into three sections. We first establish and analyze our inflationary scenarios in Sec. II. We then – in Sec. III – examine a possible post-inflationary completion of our setting. Our conclusions are summarized in Sec. IV. Throughout the text, the subscript of type z denotes derivation *with respect to* (w.r.t) the field z , and charge conjugation is denoted by a star. Unless otherwise stated, we use units where $m_{\text{P}} = 2.433 \cdot 10^{18}$ GeV is taken to be unity.

II. INFLATIONARY MODELS

In Sec. II A we describe the generic formulation of IG models within SUGRA, in Sec. II B, we construct the inflationary potential, and in Sec. II C we analyze the observational consequences of the models.

A. EMBEDDING INDUCED-GRAVITY HI IN SUGRA

The implementation of IGHI requires the determination of the relevant super- and Kähler potentials, which are specified in Sec. II A 1. In Sec. II A 2 we present the form of the action in the two relevant frames and in Sec. II A 3 we impose the IG constraint.

1. Set-up

As we already mentioned, we base the construction of our models on the superpotential

$$W_{\text{HI}} = \lambda S (\bar{\Phi}\Phi - M^2/4) \quad (1)$$

which is already introduced in the context of models of F-term hybrid inflation [24]. Here $\bar{\Phi}, \Phi$ denote a pair of left-handed chiral superfields oppositely charged under $U(1)_{B-L}$; S is a G_{B-L} -singlet chiral superfield; λ and M are parameters which can be made positive by field redefinitions. W_{HI} is the most general renormalizable superpotential consistent with a continuous R symmetry [24] under which

$$S \rightarrow e^{i\alpha} S, \bar{\Phi}\Phi \rightarrow \bar{\Phi}\Phi, W_{\text{HI}} \rightarrow e^{i\alpha} W_{\text{HI}}. \quad (2)$$

Here and in the subsequent discussion the subscript HI is frequently used instead of IGHI to simplify the notation.

As we verify below, W_{HI} allows us to break the gauge symmetry of the theory in a simple, elegant and restrictive way. The v.e.v.s of these fields, though, have to be related with the size of m_{P} according to the IG requirement. To achieve this, together with the establishment of an inflationary era, we have to combine W_{HI} with a judiciously selected Kähler potential, K . We present two classes of such K 's, which respect the (gauge and global) symmetries of W_{HI} and incorporate only quadratic terms of the various fields. We distinguish these classes taking into account the origin of the kinetic mixing in the inflaton sector. Namely:

(a) *K's without independent kinetic mixing.* Having in mind the general recipe [19, 46] for the introduction of non-minimal couplings in SUGRA we include the gauge invariant function

$$F_{\mathcal{R}} = \bar{\Phi}\Phi \quad (3)$$

in the following K 's

$$K_{1\mathcal{R}} = -N \ln \left(c_{\mathcal{R}} (F_{\mathcal{R}} + F_{\mathcal{R}}^*) - \frac{|\Phi|^2 + |\bar{\Phi}|^2}{N} + F_{1S} \right), \quad (4a)$$

which is completely logarithmic, and

$$K_{2\mathcal{R}} = -N \ln \left(c_{\mathcal{R}} (F_{\mathcal{R}} + F_{\mathcal{R}}^*) - \frac{|\Phi|^2 + |\bar{\Phi}|^2}{N} \right) + F_{2S}, \quad (4b)$$

which is polylogarithmic. In both cases we take $N > 0$. The crucial difference of the K 's considered here, compared to those employed in Ref. [19, 46], is that unity does not accompany the terms $c_{\mathcal{R}} (F_{\mathcal{R}} + F_{\mathcal{R}}^*)$. As explained in Sec. II A 3, the identification of this quantity with unity at the vacuum of the theory essentially encapsulates the IG hypothesis – cf. Ref. [3, 5]. The existence of the real function $|\Phi|^2 + |\bar{\Phi}|^2$ inside the argument of logarithm is vital for this scenario, since otherwise the Kähler metric is singular. These terms provide canonical kinetic terms for $K = K_{1\mathcal{R}}$ and $N = 3$ in the Jordan frame or $c_{\mathcal{R}}$ -dependent kinetic mixing in the remaining cases, as we show in the next Section.

(b) *K's with independent kinetic mixing.* In this case we introduce a softly broken shift symmetry for the Higgs fields – cf. Ref. [20, 31] – via the functions $F_{\pm} = |\Phi \pm \bar{\Phi}^*|^2$. In particular, the dominant shift symmetry adopted here is

$$\Phi \rightarrow \Phi + c \quad \text{and} \quad \bar{\Phi} \rightarrow \bar{\Phi} + c^* \quad \text{with} \quad c \in \mathbb{C}, \quad (5)$$

under which F_- remains unaltered whereas F_+ expresses the violation of this symmetry and is placed in the argument of a logarithm with coefficient $(-N)$, whereas F_- is set outside it. Namely, we propose the following K 's

$$K_1 = -N \ln(c_+ F_+ + F_{1S}(|S|^2)) + c_- F_-, \quad (6a)$$

$$K_2 = -N \ln(c_+ F_+) + c_- F_- + F_{2S}(|S|^2), \quad (6b)$$

$$K_3 = -N \ln(c_+ F_+) + F_{3S}(F_-, |S|^2), \quad (6c)$$

where $N > 0$. As in the case of the K 's in Eqs. (4a) and (4b) unity is not included in the argument of the logarithm. In the present case, the identification of $c_+ F_+$ with unity – see Sec. II A 3 – at the vacuum of the theory incarnates the IG hypothesis – cf. Ref. [3, 5]. The degree of the violation of the symmetry in Eq. (5) is expressed by $r_{\pm} = c_+/c_-$, which is constrained by the unification condition to values of the order 0.1 – see Sec. II B 3. Since this value is quite natural we are not forced here to invoke any argument regarding its naturalness – cf. Ref. [23].

The models employing the K 's in Eqs. (4a) and (4b) are more economical compared to the models based on the K 's in Eqs. (6a) – (6c). Indeed, the latter include two parameters (c_+ and c_-) from which one (c_+) enters $f_{\mathcal{R}}$ and the other (c_-) dominates independently the kinetic mixing – see below. However, these parameters are related to the shift symmetry in Eq. (5) which renders the relevant setting theoretically more appealing. Indeed, this symmetry has a string theoretical origin as shown in Ref. [47]. In this framework, mainly integer N 's are considered which can be reconciled with the observational data – see Sec. II C 3. Namely, $N = 3$ [$N = 2$] for $K = K_1$ [$K = K_2$ or K_3] yields completely acceptable results. However, the deviation of the N 's from these integer values is also acceptable [5, 20, 22, 23, 48] and assist us to cover the whole allowed domain of the observables.

Another possibility that could be inspected is what happens if we place the term $c_- F_-$ inside the argument of the logarithm in Eqs. (6a) and (6b) – cf. Ref. [20] – considering the Kähler potentials

$$K_{01} = -N \ln(c_+ F_+ - c_- F_-/N + F_{1S}), \quad (7a)$$

$$K_{02} = -N \ln(c_+ F_+ - c_- F_-/N) + F_{2S}. \quad (7b)$$

These K 's, though, reduce to $K_{1\mathcal{R}}$ and $K_{2\mathcal{R}}$ respectively if we set

$$c_+ = \frac{Nc_{\mathcal{R}} - 1}{2N} \quad \text{and} \quad c_- = \frac{Nc_{\mathcal{R}} + 1}{2}. \quad (8)$$

For $c_{\mathcal{R}} \gg 1$ the arrangement above results in $r_{\pm} \simeq 1/N$. On the other hand, the same r_{\pm} is found if we impose the unification constraint. Therefore, the observational predictions of the models based on the K 's above are expected to be very similar to those obtained using Eqs. (4a) and (4b).

The functions F_{lS} with $l = 1, 2, 3$ encountered in Eqs. (4a), (4b) and (6a) – (6c) support canonical normalization and safe stabilization of S during and after IGHI. Their possible forms are given in Ref. [23]. Just for definiteness, we adopt here

only their logarithmic form, i.e.,

$$F_{1S} = -\ln(1 + |S|^2/N), \quad (9a)$$

$$F_{2S} = N_S \ln(1 + |S|^2/N_S), \quad (9b)$$

$$F_{3S} = N_S \ln(1 + |S|^2/N_S + c_- F_-/N_S), \quad (9c)$$

with $0 < N_S < 6$. Recall [6, 46] that the simplest term $|S|^2$ leads to instabilities for $K = K_1$ and light excitations for $K = K_2$ and K_3 . The heaviness of these modes is required so that the observed curvature perturbation is generated wholly by our inflaton in accordance with the lack of any observational hint [53] for large non-Gaussianity in the cosmic microwave background.

2. From Einstein to Jordan Frame

With the ingredients above we can extract the part of the *Einstein frame* (EF) action within SUGRA related to the complex scalars $z^\alpha = S, \Phi, \bar{\Phi}$ – denoted by the same superfield symbol. This has the form [46]

$$S = \int d^4x \sqrt{-\hat{g}} \left(-\frac{1}{2} \hat{\mathcal{R}} + K_{\alpha\bar{\beta}} \hat{g}^{\mu\nu} D_\mu z^\alpha D_\nu z^{*\bar{\beta}} - \hat{V} \right), \quad (10a)$$

where $\hat{\mathcal{R}}$ is the EF Ricci scalar curvature, D_μ is the gauge covariant derivative, $K_{\alpha\bar{\beta}} = K_{,z^\alpha z^{*\bar{\beta}}}$, and $K^{\alpha\bar{\beta}} K_{\bar{\beta}\gamma} = \delta_\gamma^\alpha$. Also, \hat{V} is the EF SUGRA potential which can be found in terms of W_{HI} in Eq. (1) and the K 's in Eqs. (6a) – (6c) via the formula

$$\hat{V} = e^K \left(K^{\alpha\bar{\beta}} (D_\alpha W_{\text{HI}}) D_{\bar{\beta}}^* W_{\text{HI}}^* - 3|W_{\text{HI}}|^2 \right) + \frac{g^2}{2} \sum_a D_a^2, \quad (10b)$$

where $D_\alpha W_{\text{HI}} = W_{\text{HI},z^\alpha} + K_{,z^\alpha} W_{\text{HI}}$, $D_a = z^\alpha (T_a)_{\alpha}^{\beta} K_{\beta}$ and the summation is applied over the generators T_a of G_{B-L} . In the *right-hand side* (r.h.s) of the equation above we clearly recognize the contribution from the D terms (proportional to g^2) and the remaining one which comes from the F terms.

If we perform a conformal transformation, along the lines of Ref. [20, 46], defining the frame function as

$$-\Omega/N = \exp(-K/N) \Rightarrow K = -N \ln(-\Omega/N), \quad (11)$$

we can obtain the form of S in the *Jordan Frame* (JF) which is written as [20]

$$S = \int d^4x \sqrt{-g} \left(\frac{\Omega}{2N} \mathcal{R} - \frac{27}{N^3} \Omega \mathcal{A}_\mu \mathcal{A}^\mu - V + \left(\Omega_{\alpha\bar{\beta}} + \frac{3-N}{N} \frac{\Omega_\alpha \Omega_{\bar{\beta}}}{\Omega} \right) D_\mu z^\alpha D^\mu z^{*\bar{\beta}} \right), \quad (12a)$$

where we use the shorthand notation $\Omega_\alpha = \Omega_{,z^\alpha}$, and $\Omega_{\bar{\alpha}} = \Omega_{,z^{*\bar{\alpha}}}$. We also set $V = \hat{V} \Omega^2 / N^2$ and

$$\mathcal{A}_\mu = -iN (\Omega_\alpha D_\mu z^\alpha - \Omega_{\bar{\alpha}} D_\mu z^{*\bar{\alpha}}) / 6\Omega. \quad (12b)$$

Computing the expression in the parenthesis of the second line in Eq. (12a) for $K = K_{1\mathcal{R}}$ and $K_{2\mathcal{R}}$, we can easily verify that

the choice for $N = 3$ ensures canonical kinetic terms – in accordance with the findings in Ref. [19, 46] – whereas in the remaining cases a $c_{\mathcal{R}}$ - (and not ϕ -) dependent kinetic mixing emerges. Indeed, in any case we have $\Omega_{\alpha\bar{\beta}} = \delta_{\alpha\bar{\beta}}$ and for $N = 3$ the second term in the parenthesis vanishes. On the contrary, for $K = K_1, K_2$ and K_3 , the same expression is not only different than $\delta_{\alpha\bar{\beta}}$ but also includes (ϕ -dependent) entries proportional to and dominated by $c_- \gg c_+$. For this reason, the relevant models of IGHI may be more properly characterized as kinetically modified. The non-renormalizability of this kinetic mixing is under control since $\phi \ll 1$ and the theory is trustable up to m_P , as we show in Sec. II C 2.

Most importantly, though, the first term in the first line of the r.h.s of Eq. (12a) reveals that $-\Omega/N$ plays the role of a non-minimal coupling to gravity. Comparing Eq. (11) with the K 's in Eqs. (4a) – (6c) we can infer that

$$-\frac{\Omega}{N} = \begin{cases} 2(Nc_{\mathcal{R}} + 1)F_{\mathcal{R}}/N & \text{for } K = K_{1\mathcal{R}} \text{ and } K_{2\mathcal{R}}, \\ c_+F_+ & \text{for } K = K_1, K_2 \text{ and } K_3, \end{cases} \quad (13)$$

along the field configuration

$$\Phi = \bar{\Phi}^* \quad \text{and} \quad S = 0, \quad (14)$$

which is a honest inflationary trajectory, as shown in Sec. II B 2. The identification of the quantity in Eq. (13) with m_P^2 at the vacuum, according to the IG conjecture, can be accommodated as described in the next section.

3. Induced-Gravity Requirement

The implementation of the IG scenario requires the generation of m_P at the vacuum of the theory, which thereby has to be determined. To do this we have to compute V in Eq. (10b) for small values of the various fields, expanding it in powers of $1/m_P$. Namely, we obtain the following low-energy effective potential

$$V_{\text{eff}} = e^{\tilde{K}} \tilde{K}^{\alpha\bar{\beta}} W_{\text{HI}\alpha} W_{\text{HI}\bar{\beta}}^* + \frac{g^2}{2} \sum_a D_a^2 + \dots, \quad (15a)$$

where the ellipsis represents terms proportional to W_{HI} or $|W_{\text{HI}}|^2$ which obviously vanish along the path in Eq. (68) – we assume here that the vacuum is contained in the inflationary trajectory. Also, \tilde{K} is the limit of the K 's in Eqs. (4a) – (6c) for $m_P \rightarrow \infty$. The absence of unity in the arguments of the logarithms multiplied by N in these K 's prevents the drastic simplification of \tilde{K} , especially for $K = K_{1\mathcal{R}}$ and K_1 – cf. Ref. [23]. As a consequence, the expression of the resulting V_{eff} is rather lengthy. For this reason we confine ourselves below to $K = K_2$ or K_3 where F_{lS} with $l = 2, 3$ is placed outside the first logarithm and so \tilde{K} can be significantly simplified. Namely, we get

$$\tilde{K} = -N \ln c_+ F_+ + c_- F_- + |S|^2, \quad (15b)$$

from which we can then compute

$$\left(\tilde{K}^{\alpha\bar{\beta}} \right) = \text{diag} \left(\tilde{M}_{\pm}, 1 \right) \quad \text{with} \quad \tilde{M}_{\pm} = \begin{pmatrix} c_- & \tilde{K}_{\Phi\bar{\Phi}^*} \\ \tilde{K}_{\Phi\bar{\Phi}^*} & c_- \end{pmatrix}. \quad (16a)$$

Here,

$$\tilde{K}_{\Phi\bar{\Phi}^*} = \frac{N}{(\Phi + \bar{\Phi}^*)^2} \quad \text{and} \quad \tilde{K}_{\bar{\Phi}\Phi^*} = \frac{N}{(\Phi^* + \bar{\Phi})^2}, \quad (16b)$$

since

$$\tilde{K}_{\Phi} = -N/(\Phi + \bar{\Phi}^*) + c_-(\Phi^* - \bar{\Phi}) \quad (16c)$$

and

$$\tilde{K}_{\bar{\Phi}} = -N/(\Phi^* + \bar{\Phi}) - c_-(\Phi - \bar{\Phi}^*). \quad (16d)$$

To compute V_{eff} we need to know

$$\left(\tilde{K}^{\alpha\bar{\beta}} \right) = \text{diag} \left(\tilde{M}_{\pm}^{-1}, 1 \right), \quad (17a)$$

where

$$\tilde{M}_{\pm}^{-1} = \frac{1}{\det \tilde{M}_{\pm}} \begin{pmatrix} c_- & -\tilde{K}_{\Phi\bar{\Phi}^*} \\ -\tilde{K}_{\bar{\Phi}\Phi^*} & c_- \end{pmatrix}, \quad (17b)$$

with

$$\det \tilde{M}_{\pm} = c_-^2 - N^2/F_{\pm}^2. \quad (17c)$$

Upon substitution of Eqs. (17a) and (17b) into Eq. (15a) we obtain

$$V_{\text{eff}} \simeq \lambda^2 e^{\tilde{K}_+} \left| \bar{\Phi}\Phi - \frac{1}{4}M^2 \right|^2 + \frac{g^2}{2} \left(\Phi \tilde{K}_{\Phi} - \bar{\Phi} \tilde{K}_{\bar{\Phi}} \right)^2 + \frac{\lambda^2 e^{\tilde{K}_+} |S|^2}{\det \tilde{M}_{\pm}} \left(c_- (|\Phi|^2 + |\bar{\Phi}|^2) - \tilde{K}_{\Phi\bar{\Phi}^*} \bar{\Phi}^* \Phi - \tilde{K}_{\bar{\Phi}\Phi^*} \bar{\Phi} \Phi^* \right), \quad (18)$$

where $\tilde{K}_+ = -N \ln c_+ F_+$. We remark that the direction in Eq. (68) assures D-flatness since $\langle \Phi \tilde{K}_{\Phi} \rangle = \langle \bar{\Phi} \tilde{K}_{\bar{\Phi}} \rangle$ and so the vacuum lies along it with

$$\langle S \rangle = 0 \quad \text{and} \quad |\langle \Phi \rangle| = |\langle \bar{\Phi} \rangle| = M/2. \quad (19)$$

The same result holds also for $K = K_{1\mathcal{R}}, K_{2\mathcal{R}}$ and K_1 as we can verify after a more tedious computation. Eq. (19) means that $\langle \Phi \rangle$ and $\langle \bar{\Phi} \rangle$ spontaneously break $U(1)_{B-L}$ down to \mathbb{Z}_2^{B-L} . Note that $U(1)_{B-L}$ is already broken during IGHI and so no cosmic string are formed – contrary to what happens in the models of the standard F-term hybrid inflation [25, 26], which also employ W_{HI} in Eq. (1).

Inserting Eq. (19) into Eq. (13) we deduce that the conventional Einstein gravity can be recovered at the vacuum if

$$M = \begin{cases} \sqrt{2N/(Nc_{\mathcal{R}} - 1)} & \text{for } K = K_{1\mathcal{R}} \text{ and } K_{2\mathcal{R}}, \\ 1/\sqrt{c_+} & \text{for } K = K_1, K_2 \text{ and } K_3. \end{cases} \quad (20)$$

For $c_{\mathcal{R}} \simeq 10^4$ or $c_+ \sim (10^2 - 10^3)$ employed here, the resulting values of M are theoretically quite natural since they lie close to unity. Indeed, since the form of W_{HI} in Eq. (1) is established around m_P we expect that the scales entered by hand in the theory have comparable size.

B. INFLATIONARY POTENTIAL

Below we outline the derivation of the inflationary potential in Sec. II B 1 and check its stability by computing one-loop corrections in Sec. II B 2. The last part of the analysis allows us to determine the gauge-coupling unification condition (see Sec. II B 3) which assists us to further constrain our models.

1. Tree-Level Result

If we express Φ , $\bar{\Phi}$ and S according to the parametrization

$$\Phi = \frac{\phi e^{i\theta}}{\sqrt{2}} \cos \theta_\Phi, \quad \bar{\Phi} = \frac{\phi e^{i\bar{\theta}}}{\sqrt{2}} \sin \theta_\Phi \quad \text{and} \quad S = \frac{s + i\bar{s}}{\sqrt{2}}, \quad (21)$$

with $0 \leq \theta_\Phi \leq \pi/2$, the trough in Eq. (68) can be written as

$$\bar{s} = s = \theta = \bar{\theta} = 0 \quad \text{and} \quad \theta_\Phi = \pi/4. \quad (22)$$

Along this the only surviving term in Eq. (10b) is

$$\widehat{V}_{\text{HI}} = e^K K^{SS^*} |W_{\text{HI},S}|^2, \quad (23a)$$

which, for the choices of K 's in Eqs. (6a) – (6c), reads

$$\widehat{V}_{\text{HI}} = \frac{\lambda^2 f_W^2}{16a_W^2} f_{\mathcal{R}}^{-N} \cdot \begin{cases} f_{\mathcal{R}} & \text{for } K = K_{1\mathcal{R}}, K_1, \\ 1 & \text{for } K = K_{2\mathcal{R}}, K_2 \text{ and } K_3, \end{cases} \quad (23b)$$

where $f_{\mathcal{R}}^{-N} = e^K$ and we define the (inflationary) frame function as

$$f_{\mathcal{R}} = - \left. \frac{\Omega}{N} \right|_{\text{Eq. (22)}} \quad (23c)$$

which is translated as

$$f_{\mathcal{R}} = \begin{cases} (Nc_{\mathcal{R}} - 1)\phi^2/2N & \text{for } K = K_{1\mathcal{R}} \text{ and } K_{2\mathcal{R}}, \\ c_+\phi^2 & \text{for } K = K_1, K_2 \text{ and } K_3. \end{cases} \quad (23d)$$

The last factor in Eq. (23b) originates from the expression of K^{SS^*} for the various K 's. Also

$$f_W = \begin{cases} (Nc_{\mathcal{R}} - 1)\phi^2 - 2N & \text{for } K = K_{1\mathcal{R}} \text{ and } K_{2\mathcal{R}}, \\ c_+\phi^2 - 1 & \text{for } K = K_1, K_2 \text{ and } K_3, \end{cases} \quad (23e)$$

arises from the last factor in the r.h.s of Eq. (23a) together with $a_W = (Nc_{\mathcal{R}} - 1)$ for $K = K_{1\mathcal{R}}$ and $K_{2\mathcal{R}}$ and $a_W = c_+$ for $K = K_1, K_2$ and K_3 . If we set

$$N = \begin{cases} 2n + 3 & \text{for } K = K_{1\mathcal{R}}, K_1, \\ 2(n + 1) & \text{for } K = K_{2\mathcal{R}}, K_2 \text{ and } K_3, \end{cases} \quad (23f)$$

we arrive at a universal expression for \widehat{V}_{HI} which is

$$\widehat{V}_{\text{HI}} = \frac{\lambda^2 f_W^2}{16a_W^2 f_{\mathcal{R}}^{2(1+n)}}. \quad (24)$$

The value $n = 0$ is special since we get $N = 3$ for $K = K_{1\mathcal{R}}$ and K_1 or $N = 2$ for $K = K_{2\mathcal{R}}, K_2$ or K_3 . Therefore, \widehat{V}_{HI} develops an inflationary plateau as in the original case of Starobinsky model within no-scale SUGRA [3, 6] for large $c_{\mathcal{R}}$ or c_+ . Contrary to that case, though, here we also have n and c_- , whose variation may have an important impact on the observables – cf. Ref. [20, 22]. In particular, for $n < 0$, \widehat{V}_{HI} remains an increasing function of ϕ , whereas for $n > 0$, it develops a local maximum

$$\widehat{V}_{\text{HI}}(\phi_{\text{max}}) = \frac{\lambda^2 n^{2n}}{16a^2(1+n)^{2(1+n)}} \quad \text{at} \quad \phi_{\text{max}} = \sqrt{\frac{1+n}{an}}, \quad (25)$$

where $a = c_{\mathcal{R}}/2$ for $K = K_{1\mathcal{R}}$ and $K_{2\mathcal{R}}$ whereas $a = c_+$ for $K = K_1, K_2$ and K_3 . In a such case we are forced to assume that hilltop [49] IGHI occurs with ϕ rolling from the region of the maximum down to smaller values. The relevant tuning of the initial conditions can be quantified by defining [26] the quantity

$$\Delta_{\text{max}\star} = (\phi_{\text{max}} - \phi_\star) / \phi_{\text{max}}, \quad (26)$$

where ϕ_\star is the value of ϕ when the pivot scale $k_\star = 0.05/\text{Mpc}$ crosses outside the inflationary horizon. The naturalness of the attainment of IGHI increases with $\Delta_{\text{max}\star}$, and it is maximized when $\phi_{\text{max}} \gg \phi_\star$ which results in $\Delta_{\text{max}\star} \simeq 1$.

To specify the EF canonically normalized inflaton, we note that, for all choices of K in Eqs. (4a), (4b) and (6a) – (6c), $K_{\alpha\bar{\beta}}$ along the configuration in Eq. (22) takes the form

$$(K_{\alpha\bar{\beta}}) = \text{diag}(M_\pm, K_{SS^*}), \quad (27)$$

where $K_{SS^*} = 1/f_{\mathcal{R}}$ [$K_{SS^*} = 1$] for $K = K_{1\mathcal{R}}, K_1$ [$K = K_{2\mathcal{R}}, K_2$ and K_3]. For $K = K_{1\mathcal{R}}$ and $K_{2\mathcal{R}}$ we find

$$M_\pm = \begin{pmatrix} (1 + Nc_{\mathcal{R}})/2f_{\mathcal{R}} & N/\phi^2 \\ N/\phi^2 & (1 + Nc_{\mathcal{R}})/2f_{\mathcal{R}} \end{pmatrix}. \quad (28)$$

and upon diagonalization we obtain the following eigenvalues

$$\kappa_+ = Nc_{\mathcal{R}} f_{\mathcal{R}}^{-1} \quad \text{and} \quad \kappa_- = f_{\mathcal{R}}^{-1}. \quad (29)$$

Note that the existence of the real function $|\Phi|^2 + |\bar{\Phi}|^2$ inside the argument of logarithm is vital for this scenario, since otherwise M_\pm develops zero eigenvalue and so it is singular, i.e., no $K^{\alpha\bar{\beta}}$ can be defined. On the other hand, for $K = K_1, K_2$ and K_3 we obtain

$$M_\pm = \begin{pmatrix} c_- & N/\phi^2 \\ N/\phi^2 & c_- \end{pmatrix}, \quad (30)$$

with eigenvalues

$$\kappa_\pm = c_- \pm N/\phi^2. \quad (31)$$

Given that the lowest ϕ value is given in Eq. (20), we can impose, in this case, a robust restriction on the parameters to assure the positivity of κ_- during and after IGHI. Namely,

$$\kappa_- \gtrsim 0 \quad \Rightarrow \quad r_\pm \lesssim 1/N, \quad (32)$$

TABLE I: Mass-squared spectrum of the inflaton sector for $K = K_{1\mathcal{R}}, K_{2\mathcal{R}}, K_1, K_2$ and K_3 along the path in Eq. (22).

FIELDS	EIGEN-STATES	MASSES SQUARED				
			$K = K_{1\mathcal{R}}$	$K = K_{2\mathcal{R}}$	$K = K_1$	$K = K_2$
4 Real Scalars	$\hat{\theta}_+$	$\hat{m}_{\theta_+}^2$	$6\hat{H}_{\text{HI}}^2(1 - 1/N)$	$6\hat{H}_{\text{HI}}^2$	$6\hat{H}_{\text{HI}}^2$	$6(1 + 1/N_S)\hat{H}_{\text{HI}}^2$
	$\hat{\theta}_\Phi$	$\hat{m}_{\theta_\Phi}^2$	$M_{BL}^2 + 6\hat{H}_{\text{HI}}^2 c_{\mathcal{R}}(N - 3)$	$M_{BL}^2 + 6\hat{H}_{\text{HI}}^2 c_{\mathcal{R}}(N - 2)$	$M_{BL}^2 + 6\hat{H}_{\text{HI}}^2$	$M_{BL}^2 + 6(1 + 1/N_S)\hat{H}_{\text{HI}}^2$
	$\hat{s}, \hat{\bar{s}}$	\hat{m}_s^2	$3\hat{H}_{\text{HI}}^2(N - 6 + c_{\mathcal{R}}\phi^2/N)$	$3\hat{H}_{\text{HI}}^2(4/N - 4 + N + 2/N_S)$	$6f_W\hat{H}_{\text{HI}}^2/N$	$6\hat{H}_{\text{HI}}^2/N_S$
1 Gauge Boson	A_{BL}	M_{BL}^2	$2Ng^2/(Nc_{\mathcal{R}} - 1)$		$g^2(c_- \phi^2 - N)$	
4 Weyl Spinors	$\hat{\psi}_\pm$	$\hat{m}_{\psi_\pm}^2$	$3\hat{H}_{\text{HI}}^2(c_{\mathcal{R}}(N - 2)\phi^2 - 2N)^2/N^2 c_{\mathcal{R}}^2 \phi^4$		$6(N - c_+(N - 2)\phi^2)^2 \hat{H}_{\text{HI}}^2/c_- f_W^2 \phi^2$	
	$\lambda_{BL}, \hat{\psi}_{\Phi-}$	M_{BL}^2	$2Ng^2/(Nc_{\mathcal{R}} - 1)$		$g^2(c_- \phi^2 - N)$	

whereas we are not obliged to impose any condition for $K = K_{1\mathcal{R}}$ and $K_{2\mathcal{R}}$.

Inserting Eqs. (21) and (30) in the second term of the r.h.s of Eq. (10a) we can define the EF canonically normalized fields, denoted by hat, as follows

$$\frac{d\hat{\phi}}{d\phi} = J = \sqrt{\kappa_+}, \quad \hat{\theta}_+ = \frac{J\phi\theta_+}{\sqrt{2}}, \quad \hat{\theta}_- = \sqrt{\frac{\kappa_-}{2}}\phi\theta_-, \quad (33a)$$

$$\hat{\theta}_\Phi = \phi\sqrt{\kappa_-}(\theta_\Phi - \pi/4), \quad (\hat{s}, \hat{\bar{s}}) = \sqrt{K_{SS^*}}(s, \bar{s}), \quad (33b)$$

where $\theta_\pm = (\bar{\theta} \pm \theta)/\sqrt{2}$. Note, in passing, that the spinors ψ_S and $\psi_{\Phi\pm}$ associated with the superfields S and $\Phi - \bar{\Phi}$ are similarly normalized, i.e., $\hat{\psi}_S = \sqrt{K_{SS^*}}\psi_S$ and $\hat{\psi}_{\Phi\pm} = \sqrt{\kappa_\pm}\psi_{\Phi\pm}$ with $\psi_{\Phi\pm} = (\psi_\Phi \pm \psi_{\bar{\Phi}})/\sqrt{2}$.

2. Stability and Loop-Corrections

We can verify that the inflationary direction in Eq. (22) is stable w.r.t the fluctuations of the non-inflaton fields. To this end, we construct the mass-squared spectrum of the various scalars defined in Eqs. (33a) and (33b). Taking the limit $c_- \gg c_+$ we find the expressions of the masses squared $\hat{m}_{\chi^\alpha}^2$ (with $\chi^\alpha = \theta_+, \theta_\Phi$ and S) arranged in Table I. For $\phi \simeq \phi_*$ these fairly approach the quite lengthy, exact expressions taken into account in our numerical computation. Given that $\phi < 0.1$ for $K = K_{1\mathcal{R}}$ and $f_W \gg 1$ for $K = K_1$ we deduce that $\hat{m}_s^2 > 0$ for $N \simeq 3$. Also for $K = K_{2\mathcal{R}}, K_2$ or K_3 and $0 < N_S < 6$, $\hat{m}_s^2 > 0$ stays positive and heavy enough, i.e. $\hat{m}_{z^\alpha}^2 \gg \hat{H}_{\text{HI}}^2 = \hat{V}_{\text{HI}}/3$. In Table I we also display the masses, M_{BL} , of the gauge boson A_{BL} – which signals the fact that G_{B-L} is broken during IGHI – and the masses of the corresponding fermions. Note that the unspecified eigestate $\hat{\psi}_\pm$ is defined as

$$\hat{\psi}_\pm = (\hat{\psi}_{\Phi+} \pm \hat{\psi}_S)/\sqrt{2}. \quad (34)$$

As a consequence, let us again emphasize that no cosmic string are produced at the end of IGHI.

The derived mass spectrum can be employed in order to find the one-loop radiative corrections, $\Delta\hat{V}_{\text{HI}}$, to \hat{V}_{HI} . Considering

SUGRA as an effective theory with cutoff scale equal to m_P , the well-known Coleman-Weinberg formula [50] can be employed taking into account only the masses which lie well below m_P , i.e., all the masses arranged in Table I besides M_{BL} and \hat{m}_{θ_Φ} – note that these contributions are cancelled out for $K = K_{1\mathcal{R}}$ and $N = 3$ or $K = K_{2\mathcal{R}}$ and $N = 2$. The resulting $\Delta\hat{V}_{\text{HI}}$ leaves intact our inflationary outputs, provided that the renormalization-group mass scale Λ , is determined by requiring $\Delta\hat{V}_{\text{HI}}(\phi_*) = 0$ or $\Delta\hat{V}_{\text{HI}}(\phi_f) = 0$. These conditions yield $\Lambda \simeq 3.2 \cdot 10^{-5} - 1.4 \cdot 10^{-4}$ and render our results practically independent of Λ since these can be derived exclusively by using \hat{V}_{HI} in Eq. (24) with the various quantities evaluated at Λ – cf. Ref. [20]. Note that their renormalization-group running is expected to be negligible because Λ is close to the inflationary scale $\hat{V}_{\text{HI}}^{1/4} \simeq (3 - 7) \cdot 10^{-3}$. Recall, here, that in the case of F-term hybrid inflation [24–27] the SUSY potential is classically flat and the radiative corrections contribute (together with the SUGRA corrections) in the inclination of the inflationary path.

3. SUSY Gauge Coupling Unification

The mass M_{BL} listed in Table I of the gauge boson A_{BL} may, in principle, be a free parameter since the $U(1)_{B-L}$ gauge symmetry does not disturb the unification of the MSSM gauge coupling constants. To be more specific, though, we prefer to determine M_{BL} by requiring that it takes the value M_{GUT} dictated by this unification at the vacuum of the theory. Namely, we impose

$$\langle M_{BL} \rangle = M_{\text{GUT}} \simeq 2/2.43 \cdot 10^{-2} = 8.22 \cdot 10^{-3}. \quad (35)$$

This simple principle has important consequences for both classes of models considered here. In particular:

(a) For $K = K_{1\mathcal{R}}$ or $K_{2\mathcal{R}}$. In this cases, the condition above completely determines $c_{\mathcal{R}}$ since it implies via the findings of Table I

$$c_{\mathcal{R}} = \frac{1}{N} + \frac{2g^2}{M_{\text{GUT}}^2} \simeq 1.451 \cdot 10^4, \quad (36)$$

leading to $M \simeq 0.0117$ via Eq. (20). Here we take $g \simeq 0.7$ which is the value of the unified coupling constant within MSSM. Although $c_{\mathcal{R}}$ above is very large, there is no problem with the validity of the effective theory, in accordance with the results of earlier works [3, 5, 11] on IG inflation with gauge singlet inflaton. Indeed, expanding about $\langle \phi \rangle = M$ – see Eq. (20) – the second term in the r.h.s of Eq. (10a) for $\mu = \nu = 0$ and \widehat{V}_{HI} in Eq. (24) we obtain

$$J^2 \dot{\phi}^2 \simeq \left(1 - \sqrt{\frac{2}{N}} \widehat{\delta\phi} + \frac{3}{2N} \widehat{\delta\phi}^2 - \sqrt{\frac{2}{N^3}} \widehat{\delta\phi}^3 + \dots \right) \widehat{\delta\phi}^2, \quad (37a)$$

where $\widehat{\delta\phi}$ is the canonically normalized inflaton at the vacuum – see Sec. III C 1 – and

$$\widehat{V}_{\text{HI}} \simeq \frac{\lambda^2 \widehat{\delta\phi}^2}{2N c_{\mathcal{R}}^2} \left(1 - \frac{2N-1}{\sqrt{2N}} \widehat{\delta\phi} + \frac{8N^2-4N+1}{8N} \widehat{\delta\phi}^2 + \dots \right). \quad (37b)$$

These expressions indicate that $\Lambda_{\text{UV}} = m_{\text{P}}$, since $c_{\mathcal{R}}$ does not appear in any of their numerators. Although these expansions are valid only during reheating we consider Λ_{UV} extracted this way as the overall cut-off scale of the theory since reheating is regarded [15] as an unavoidable stage of IGHI.

(b) For $K = K_1, K_2$ or K_3 . In this cases, the condition above allows us to fix r_{\pm} since, substituting Eq. (20) in M_{BL} shown in Table I, we obtain

$$g^2 (c_- \langle \phi \rangle^2 - N) = M_{\text{GUT}}^2 \Rightarrow r_{\pm} = \frac{g^2}{N g^2 + M_{\text{GUT}}^2}. \quad (38)$$

Since $M_{\text{GUT}} > 0$ the condition above satisfies the restriction in Eq. (32) yielding r_{\pm} close to its upper bound because $M_{\text{GUT}} \ll 1$.

As a bottom line, under the assumption in Eq. (35), $c_{\mathcal{R}}$ for $K = K_{1\mathcal{R}}$ and $K_{2\mathcal{R}}$ or r_{\pm} for $K = K_1, K_2$ and K_3 cease to be free parameters, in sharp contrast to the models of Ref. [19–23] where the same assumption is employed to extract $M \ll 1$ as a function of the free parameters without any other theoretical constraint between them. Therefore, the interplay of Eqs. (20) and (38) leads to the reduction of the free parameters by one, thereby rendering the present set-up more restrictive and predictive.

C. INFLATION ANALYSIS

In Secs. II C 2 and II C 3 below we inspect analytically and numerically respectively, if the potential in Eq. (24) endowed with the condition of Eqs. (20) and (38) may be consistent with a number of observational constraints introduced in Sec. II C 1.

1. General Framework

Given that the analysis of inflation in both EF and JF yields equivalent results [9], we carry it out exclusively in the EF. In

particular, the period of slow-roll IGHI is determined in the EF by the condition

$$\max\{\widehat{\epsilon}(\phi), |\widehat{\eta}(\phi)|\} \leq 1, \quad (39a)$$

where the slow-roll parameters [51],

$$\widehat{\epsilon} = \left(\widehat{V}_{\text{HI},\widehat{\phi}} / \sqrt{2\widehat{V}_{\text{HI}}} \right)^2 \quad \text{and} \quad \widehat{\eta} = \widehat{V}_{\text{HI},\widehat{\phi}\widehat{\phi}} / \widehat{V}_{\text{HI}}. \quad (39b)$$

The number of e-foldings \widehat{N}_{\star} that the scale $k_{\star} = 0.05/\text{Mpc}$ experiences during IGHI and the amplitude A_{s} of the power spectrum of the curvature perturbations generated by ϕ can be computed using the standard formulae [51]

$$\widehat{N}_{\star} = \int_{\widehat{\phi}_{\text{f}}}^{\widehat{\phi}_{\star}} d\widehat{\phi} \frac{\widehat{V}_{\text{HI}}}{\widehat{V}_{\text{HI},\widehat{\phi}}} \quad \text{and} \quad A_{\text{s}}^{1/2} = \frac{1}{2\sqrt{3}\pi} \frac{\widehat{V}_{\text{HI}}^{3/2}(\widehat{\phi}_{\star})}{|\widehat{V}_{\text{HI},\widehat{\phi}}(\widehat{\phi}_{\star})|}, \quad (40)$$

where $\phi_{\star} [\widehat{\phi}_{\star}]$ is the value of ϕ [$\widehat{\phi}$] when k_{\star} crosses the inflationary horizon. These observables are to be confronted with the requirements [53]

$$\widehat{N}_{\star} \simeq 61.5 + \ln \frac{\widehat{V}_{\text{HI}}(\phi_{\star})^{1/2}}{\widehat{V}_{\text{HI}}(\phi_{\text{f}})^{1/4}} + \frac{1}{2} f_{\mathcal{R}}(\phi_{\star}); \quad (41a)$$

$$A_{\text{s}}^{1/2} \simeq 4.627 \cdot 10^{-5}. \quad (41b)$$

Note that in Eq. (41a) we consider an equation-of-state parameter $w_{\text{int}} = 1/3$ corresponding to quartic potential which is expected to approximate \widehat{V}_{HI} rather well for $\phi \ll 1$ – see Ref. [20]. We obtain $\widehat{N}_{\star} \simeq (57.5 - 60)$.

Then, we compute the remaining inflationary observables, i.e., the (scalar) spectral index n_{s} , its running a_{s} , and the scalar-to-tensor ratio r which are found from the relations [51]

$$n_{\text{s}} = 1 - 6\widehat{\epsilon}_{\star} + 2\widehat{\eta}_{\star}, \quad r = 16\widehat{\epsilon}_{\star}, \quad (42a)$$

$$a_{\text{s}} = 2(4\widehat{\eta}_{\star}^2 - (n_{\text{s}} - 1)^2) / 3 - 2\widehat{\xi}_{\star}, \quad (42b)$$

where the variables with subscript \star are evaluated at $\phi = \phi_{\star}$ and $\widehat{\xi} = \widehat{V}_{\text{HI},\widehat{\phi}\widehat{\phi}\widehat{\phi}} / \widehat{V}_{\text{HI}}^2$.

The resulting values of n_{s} and r must be in agreement with the fitting of the data [13, 33] with $\Lambda\text{CDM}+r$ model. We take into account the data from *Planck* and *Baryon Acoustic Oscillations* (BAO) and the BK14 data taken by the BICEP2/Keck Array CMB polarization experiments up to and including the 2014 observing season. The results are

$$(a) \ n_{\text{s}} = 0.968 \pm 0.009 \quad \text{and} \quad (b) \ r \leq 0.07, \quad (43)$$

at 95% confidence level (c.l.) with $|a_{\text{s}}| \ll 0.01$.

2. Analytic Results

A crucial difference of the present analysis w.r.t that for the models in Ref. [19–23] is that M , given by Eq. (20), is not negligible during the inflationary period and enters the relevant formulas via the function f_{W} defined below Eq. (23b). We find it convenient to expose separately our results for the two basic classes of models introduced in Sec. II A 1. Namely:

(a) For $K = K_{1\mathcal{R}}$ and $K_{2\mathcal{R}}$. The slow-roll parameters can be derived employing J in Eq. (24), without explicitly expressing \widehat{V}_{HI} in terms of $\widehat{\phi}$. Our results are

$$\widehat{\epsilon} = 4 \frac{\widetilde{f}_{\text{W}}^2 (n\widetilde{f}_{\text{W}} - 2)^2}{N c_{\mathcal{R}}^4 \phi^8} \quad \text{and} \quad \widehat{\eta} = 8 \frac{2 - \widetilde{f}_{\text{W}} - 4n\widetilde{f}_{\text{W}} + n^2 \widetilde{f}_{\text{W}}^2}{N \widetilde{f}_{\text{W}}^2}, \quad (44)$$

where $\widetilde{f}_{\text{W}} = c_{\mathcal{R}} \phi^2 - 2$. The condition Eq. (39a) is violated for $\phi = \phi_{\text{f}}$, which is found to be

$$\phi_{\text{f}} \simeq \max \left(\frac{2}{\sqrt{c_{\mathcal{R}}}} \sqrt{\frac{1+n}{2n+\sqrt{N}}}, 2\sqrt{\frac{2}{c_{\mathcal{R}}}} \sqrt{\frac{1-4n}{8n^2+N}} \right). \quad (45)$$

Then, \widehat{N}_{\star} can be also computed from Eq. (40) as follows

$$\widehat{N}_{\star} \simeq \begin{cases} N c_{\mathcal{R}} \phi_{\star}^2 / 8 & \text{for } n = 0, \\ N \ln \left(\frac{2(1+n)}{2-n\widetilde{f}_{\text{W}\star}} \right) / 4n(1+n) & \text{for } n \neq 0, \end{cases} \quad (46)$$

where $\widetilde{f}_{\text{W}\star} = \widetilde{f}_{\text{W}}(\widehat{\phi}_{\star})$. Solving the above equations w.r.t ϕ_{\star} we obtain a unified expression

$$\phi_{\star} \simeq \sqrt{\frac{2f_{\mathcal{R}\star}}{c_{\mathcal{R}}}} \quad \text{with} \quad f_{\mathcal{R}\star} = \frac{1+n}{n} \left(1 - e^{-4n(1+n)\widehat{N}_{\star}/N} \right) \quad (47)$$

reducing to $4\widehat{N}_{\star}/N$ in the limit $n \rightarrow 0$. For $c_{\mathcal{R}}$ in Eq. (36) we can verify that $\phi_{\star} \sim 0.1$ and so the model is (automatically) well stabilized against corrections from higher order terms of the form $(\Phi\overline{\Phi})^p$ with $p > 1$ in W_{HI} – see Eq. (1). Thanks to Eq. (36), we can derive uniquely λ from the expression

$$\lambda = 8\sqrt{6A_s\pi c_{\mathcal{R}} f_{\mathcal{R}\star}^{n+1}} \frac{n(1-f_{\mathcal{R}\star})+1}{\sqrt{N}(f_{\mathcal{R}\star}-1)^2}, \quad (48)$$

applying the second equation in Eq. (40). Upon substitution of $f_{\mathcal{R}\star}$ into Eq. (42a) we obtain the predictions of the model which are

$$n_s \simeq 1 - \frac{8n^2}{N} + \frac{16}{N} \frac{n}{f_{\mathcal{R}\star}-1} - \frac{8}{N} \frac{f_{\mathcal{R}\star}+1}{(f_{\mathcal{R}\star}-1)^2}, \quad (49a)$$

$$r \simeq \frac{64}{N} \left(\frac{1+n(1-f_{\mathcal{R}\star})}{f_{\mathcal{R}\star}-1} \right)^2. \quad (49b)$$

Since only $|n| \ll 1$ are allowed, as we see below, the results above, together with a_s , can be further simplified as follows

$$n_s \simeq 1 - \frac{2}{\widehat{N}_{\star}} - \frac{4n}{N} - \frac{8n^2 \widehat{N}_{\star}}{3N^2}, \quad (50a)$$

$$r \simeq \frac{4N}{\widehat{N}_{\star}^2} - \frac{16n^3}{N} + \frac{80n^2}{3N} - \frac{64n^3 \widehat{N}_{\star}}{3N^2}, \quad (50b)$$

$$a_s \simeq -\frac{2}{\widehat{N}_{\star}^2} + \frac{3n}{\widehat{N}_{\star}^2} + \frac{8n^2}{3N^2} - \frac{7N}{2\widehat{N}_{\star}^3}, \quad (50c)$$

where, for $n = 0$, the well-known predictions of the Starobinsky model are recovered, i.e., $n_s \simeq 0.966$ and $r = 0.0032$ [$r = 0.0022$] for $K = K_{1\mathcal{R}}$ [$K = K_{2\mathcal{R}}$]. On the other hand, contributions proportional to \widehat{N}_{\star} can be tamed for sufficiently low n as we can verify numerically.

(b) For $K = K_1, K_2$ and K_3 . Working along the lines of the previous paragraph we estimate the slow-roll parameters as follows

$$\widehat{\epsilon} = \frac{8(1+n-nc_+\phi^2)^2}{c_-\phi^2 f_{\text{W}}^2}; \quad (51a)$$

$$\widehat{\eta} = \frac{5+9n-(3+10n)c_+\phi^2+4n^2 f_{\text{W}}^2+nc_+^2 \phi^2}{4c_-\phi^2 f_{\text{W}}^2}. \quad (51b)$$

Given that $\phi \ll 1$, Eq. (39a) is saturated at the maximal ϕ value, ϕ_{f} , from the following two values

$$\phi_{1\text{f}} \simeq \sqrt{\frac{2}{c_-}} \frac{1}{r_{\pm}^{1/3}} \quad \text{and} \quad \phi_{2\text{f}} \simeq \sqrt{\frac{2}{c_-}} \left(\frac{3}{r_{\pm}} \right)^{1/4}, \quad (52)$$

where $\phi_{1\text{f}}$ and $\phi_{2\text{f}}$ are such that $\widehat{\epsilon}(\phi_{1\text{f}}) \simeq 1$ and $\widehat{\eta}(\phi_{2\text{f}}) \simeq 1$. The n dependence is not so crucial for this estimation. Since $\phi_{\star} \gg \phi_{\text{f}}$, from Eq. (40) we find

$$\widehat{N}_{\star} \simeq \begin{cases} c_-\phi_{\star}^2 (c_-r_{\pm}\phi_{\star}^2/2-1)/8 & \text{for } n=0, \\ -\left(nc_+\phi_{\star}^2 + \ln\left(1-\frac{nc_+\phi_{\star}^2}{1+n}\right) \right) / 8n^2 r_{\pm} & \text{for } n \neq 0, \end{cases} \quad (53)$$

where $\widehat{\phi}_{\star}$ is the value of $\widehat{\phi}$ when k_{\star} crosses the inflationary horizon. As regards the consistency of the relation above for $n > 0$, we note that we get $nc_+\phi_{\star}^2 < 1+n$ in all relevant cases and so, $\ln(1-nc_+\phi_{\star}^2/(1+n)) < 0$ assures the positivity of \widehat{N}_{\star} . Solving the equations above w.r.t ϕ_{\star} , we can express ϕ_{\star} in terms of \widehat{N}_{\star} as follows

$$\phi_{\star} \simeq \frac{f_{\mathcal{R}\star}^{1/2}}{c_{\pm}^{1/2}} \quad \text{with} \quad f_{\mathcal{R}\star} = \begin{cases} 1 + \left(1 + 16r_{\pm}\widehat{N}_{\star} \right)^{1/2} & \text{for } n=0, \\ (1+n+W_k(y))/n & \text{for } n \neq 0, \end{cases} \quad (54)$$

where we make use of Eq. (23d). Also, W_k is the Lambert W (or product logarithmic) function [52] with

$$y = -(1+n) \exp\left(-1-n(1+8n\widehat{N}_{\star}r_{\pm})\right). \quad (55)$$

We take $k = 0$ for $n > 0$ and $k = -1$ for $n < 0$.

Contrary to what happens for $K = K_{1\mathcal{R}}$ and $K_{2\mathcal{R}}$, c_- is not uniquely determined here. Therefore, for any n we are obliged to impose a lower bound on it, above which $\phi_{\star} \leq 1$. Indeed, from Eq. (54) we have

$$\phi_{\star} \leq 1 \Rightarrow c_- \geq f_{\mathcal{R}\star}/r_{\pm}, \quad (56)$$

and so our proposal can be stabilized against corrections from higher order terms. Despite the fact that c_- may take relatively large values, the corresponding effective theories are valid [14, 15] up to $m_{\text{P}} = 1$ for r_{\pm} given by Eq. (38). To further clarify this point we have to identify the ultraviolet cut-off scale Λ_{UV} of the theory by analyzing the small-field behavior of our models. More specifically, adapting the expansions in Eqs. (37a) and (37b) in our present case, we end up with the expressions

$$J^2 \dot{\phi}^2 \simeq \left(1 - 2\bar{r}_{\pm}^3 \widehat{\delta\phi} + 3N\bar{r}_{\pm}^4 \widehat{\delta\phi}^2 - 4N\bar{r}_{\pm}^5 \widehat{\delta\phi}^3 + \dots \right) \widehat{\delta\phi}^2, \quad (57a)$$

where we set $\bar{r}_\pm = \sqrt{r_\pm/(1 + Nr_\pm)}$, and

$$\widehat{V}_{\text{HI}} \simeq \frac{\lambda^2 \bar{r}_\pm^2 \widehat{\phi}^2}{4c_+^2} \left(1 - (3 + 4n)\bar{r}_\pm \widehat{\phi} + \left(\frac{25}{4} + 14n + 8n^2 \right) \bar{r}_\pm^2 \widehat{\phi}^2 + \dots \right). \quad (57b)$$

From the expressions above we conclude that $\Lambda_{\text{UV}} = m_{\text{P}}$ since $r_\pm \leq 1$ (and so $\bar{r}_\pm \leq 1$) due to Eq. (38).

From the second equation in Eq. (40) we can also conclude that λ is proportional to c_- for fixed n . Indeed, plugging Eq. (54) into this equation and solving w.r.t λ , we find

$$\lambda = 32\sqrt{3A_s\pi c_-} r_\pm^{3/2} f_{\mathcal{R}_*}^{n+1/2} \frac{n(1 - f_{\mathcal{R}_*}) + 1}{(f_{\mathcal{R}_*} - 1)^2}. \quad (58)$$

Numerically, – see below – we find that λ/c_- develops a maximum at $n \simeq -0.15$ which signals a transition to a branch of inflationary solutions which deviate from those obtained within the Starobinsky-like inflation.

Inserting $f_{\mathcal{R}_*}$ from Eq. (54) into Eqs. (42a) and (42b) we obtain

$$n_s \simeq 1 - \frac{8}{f_{\mathcal{R}_*}} \left(\frac{3f_{\mathcal{R}_*} + 1}{(f_{\mathcal{R}_*} - 1)^2} - n \frac{f_{\mathcal{R}_*} + 3}{f_{\mathcal{R}_*} - 1} + 2n^2 \right), \quad (59a)$$

$$r \simeq 128 \frac{r_\pm}{f_{\mathcal{R}_*}} \left(\frac{1 - n(f_{\mathcal{R}_*} - 1)}{f_{\mathcal{R}_*} - 1} \right)^2, \quad (59b)$$

$$a_s \simeq \frac{64r_\pm^2}{3(f_{\mathcal{R}_*} - 1)^4 f_{\mathcal{R}_*}^2} \left(3 - 9f_{\mathcal{R}_*}(2f_{\mathcal{R}_*} + 1) + 3(f_{\mathcal{R}_*} - 1)(f_{\mathcal{R}_*}(7f_{\mathcal{R}_*} + 9) - 4)n + 2(f_{\mathcal{R}_*} - 1)^2(f_{\mathcal{R}_*}(f_{\mathcal{R}_*} - 42) + 121)n^2 \right). \quad (59c)$$

where we can recognize the similarities with the formulas given in Eqs. (49a) and (49b). For $|n| < 0.1$ these formulas may be expanded successively in series of n and $1/\widehat{N}_*$ with results

$$n_s \simeq 1 - \frac{16}{3}n^2 r_\pm - 2n \frac{r_\pm^{1/2}}{\widehat{N}_*^{1/2}} - \frac{3 - 2n}{2\widehat{N}_*} - \frac{3 + 5n}{24(\widehat{N}_*^3 r_\pm)^{1/2}}, \quad (60a)$$

$$r \simeq -\frac{8n}{\widehat{N}_*} - \frac{1}{2\widehat{N}_*^2 r_\pm} + \frac{2(3 + 2n)}{3(\widehat{N}_*^3 r_\pm)^{1/2}} + \frac{32n^2 r_\pm^{1/2}}{3\widehat{N}_*^{1/2}}, \quad (60b)$$

$$a_s \simeq -\frac{nr_\pm^{1/2}}{\widehat{N}_*^{3/2}} - \frac{3 - 2n}{2\widehat{N}_*^2}. \quad (60c)$$

From the expressions above, we can infer that there is a clear n (and r_\pm) dependence of the observables which deviate somewhat from those obtained in the pure Starobinsky-type inflation (or IG inflation) [3, 5, 6]. Note that the formulae, although similar, are not identical with those found in Ref. [23].

3. Numerical Results

The approximate analytic expressions above can be verified by the numerical analysis. Namely, we apply the accurate expressions in Eq. (40) and confront them with the requirements

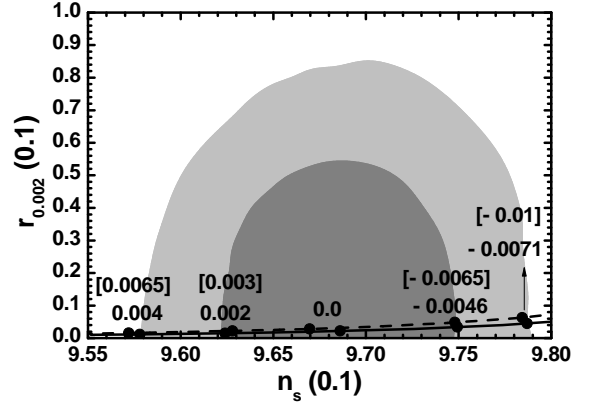


FIG. 1: Allowed curves in the $n_s - r_{0.002}$ plane for $K = K_{1\mathcal{R}}$ (dashed line) and $K = K_{2\mathcal{R}}$ (solid line) – the n values in [outside] squared brackets correspond to $K = K_{1\mathcal{R}}$ [$K = K_{2\mathcal{R}}$]. The marginalized joint 68% [95%] regions from Planck, BAO and BK14 data are depicted by the dark [light] shaded contours.

in Eqs. (41a) – (41b) adjusting $c_{\mathcal{R}}$ and λ for $K = K_{1\mathcal{R}}$ and $K_{2\mathcal{R}}$ or c_- and λ for with any selected n . Then, we compute the model predictions via Eqs. (42a) and (42b). Our results are mainly displayed in Figs. 1 and 2, where we show a comparison of the models' predictions against the observational data [13, 33] in the $n_s - r_{0.002}$ plane, where $r_{0.002} = 16\widehat{e}(\widehat{\phi}_{0.002})$ with $\widehat{\phi}_{0.002}$ being the value of $\widehat{\phi}$ when the scale $k = 0.002/\text{Mpc}$, which undergoes $\widehat{N}_{0.002} = \widehat{N}_* + 3.22$ e-foldings during IGHI, crosses the horizon of IGHI. Let us discuss separately the results for the two classes of models. In particular:

(a) For $K = K_{1\mathcal{R}}$ and $K_{2\mathcal{R}}$. We depict in Fig. 1 by a dashed [solid] line the model predictions for $K = K_{1\mathcal{R}}$ [$K = K_{2\mathcal{R}}$] against the observational data. We see that the whole observationally favored range at low r 's is covered varying n which remains, though, rather close to zero. In fact n is tuned closer to zero and r is slightly lower compared to those obtained for $K = K_1, K_2$ and K_3 – see below. More explicitly, we find the allowed ranges

$$0.9 \gtrsim n/0.01 \gtrsim -1 \quad \text{and} \quad 1.5 \lesssim r/10^{-3} \lesssim 6.6 \quad (61a)$$

for $K = K_{1\mathcal{R}}$, whereas for $K = K_{2\mathcal{R}}$ we have

$$5.1 \gtrsim n/0.001 \gtrsim -9 \quad \text{and} \quad 1.1 \lesssim r/10^{-3} \lesssim 5.9. \quad (61b)$$

As n varies in its allowed ranges presented below, we obtain

$$2.3 \lesssim \lambda/0.1 \lesssim 4 \quad \text{or} \quad 1.9 \lesssim \lambda/0.1 \lesssim 3.5, \quad (62)$$

for $K = K_{1\mathcal{R}}$ or $K = K_{2\mathcal{R}}$ respectively. If we take $n = 0$, we find the central values of λ in the ranges above which are 0.29 and 0.24 correspondingly.

(b) For $K = K_1, K_2$ and K_3 . In this case, let us clarify that the (theoretically) free parameters of our models are n

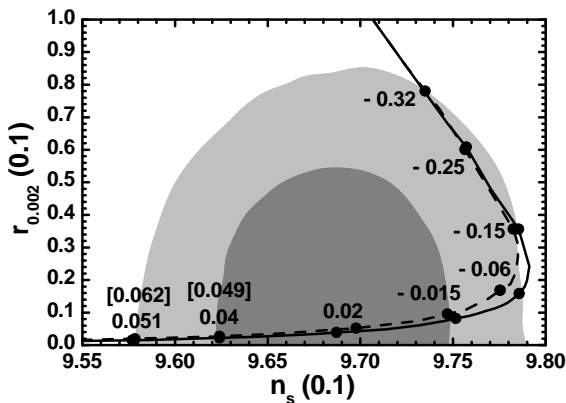


FIG. 2: The same as Fig. 1 but for $K = K_1$ (dashed line) and $K = K_2$ or K_3 (solid line) with the n values indicated on the curves (the n values in squared brackets correspond to $K = K_1$).

and λ/c_- and not n , c_- , and λ as naively expected – recall that M and r_{\pm} are found from Eqs. (20) and (38). Indeed, if we perform the rescalings

$$\Phi \rightarrow \Phi/\sqrt{c_-}, \quad \bar{\Phi} \rightarrow \bar{\Phi}/\sqrt{c_-} \quad \text{and} \quad S \rightarrow S, \quad (63)$$

V_{HI} in Eq. (1) depends on λ/c_- and r_{\pm}^{-1} , while the K 's in Eq. (6a) – (6c) depend on n and r_{\pm} . As a consequence, \hat{V}_{HI} depends exclusively on λ/c_- and n . Since the λ/c_- variation is rather trivial – see Eq. (58) – we focus below on the variation of n .

In Fig. 2 we depict the theoretically allowed values with solid and dashed lines for $K = K_2$ or K_3 and $K = K_1$ respectively. The variation of n is shown along each line. In squared brackets we display the n values for $K = K_1$ when these differ appreciably from those for $K = K_2$ or K_3 . We remark that for $n > 0$ there is a discrepancy of about 20% changing K from K_1 to K_2 or K_3 , which decreases as n decreases below zero. This effect originates from the difference in J – see Eqs. (31) and (33a) – which becomes smaller and smaller as n decreases or c_- increases. We observe that $n > 0$ values dominate the part of the curves with lower r values and $n_s \leq 0.973$, whereas the $n < 0$ values generate the part of the curves with n_s close to its upper bound in Eq. (43) and appreciably larger r values. Roughly speaking, the displayed curves can be produced interconnecting the limiting points of the various curves in Fig. 2-(a) of Ref. [23], although the curves for $0 < n < 0.1$ and $n < -0.1$ are not depicted there. This is because the r_{\pm} 's resulting from Eq. (38) are close to their upper limits induced by Eq. (32).

Comparing these theoretical outputs with data depicted by the dark [light] shaded contours at 68% c.l. [95% c.l.] we find the allowed ranges. Especially, for $K = K_1$ we obtain

$$0.62 \gtrsim n/0.1 \gtrsim -3.2, \quad 3.2 \lesssim r_{\pm}/0.1 \lesssim 4.16. \quad (64)$$

On the other hand, for $K = K_2$ or K_3 , we find one branch localized in the ranges

$$0.51 \gtrsim n/0.1 \gtrsim -0.6, \quad 4.76 \lesssim r_{\pm}/0.1 \lesssim 5.32, \quad (65)$$

TABLE II: Parameters and observables for the points shown in Fig. 2 with $K = K_2$ and K_3 .

$n/0.1$	$r_{\pm}/0.1$	$\lambda/10^{-5}c_-$	$n_s/0.1$	$-a_s/10^{-4}$	$r/0.01$
0.51	4.76	1.7	9.58	5.2	0.17
0.4	4.81	2	9.62	5.2	0.25
0.2	4.9	2.55	9.69	5	0.43
-0.15	5.07	3.4	9.75	4.5	0.88
-0.6	5.32	4.1	9.78	3.5	1.7
-1.5	5.88	4.5	9.78	3.98	3.7
-2.5	6.66	3.9	9.76	4	6.3
-3.2	7.35	3.3	9.73	4.4	8.3

and another one

$$-1.5 \gtrsim n/0.1 \gtrsim -3.2, \quad 5.88 \lesssim r_{\pm}/0.1 \lesssim 7.35. \quad (66)$$

The findings for $K = K_2$ or K_3 , can also be read-off from Table II where we list the values of the input parameter (n) depicted in Fig. 2, the corresponding output parameters (r_{\pm} and λ/c_-) and the inflationary observables. We observe that n_s and r are well confined in the allowed regions of Eq. (43), while a_s varies in the range $-(3.98 - 5.2) \cdot 10^{-4}$ and so, our models are consistent with the fitting of data with the $\Lambda\text{CDM}+r$ model [13]. Comparing these numerical values with those obtained by the analytic expressions in Eqs. (59a) – (59c) we obtain complete agreement for any n . On the other hand, the approximate formulas in Eqs. (60a) – (60c) are valid only for $|n_s| < 0.1$, i.e., the Starobinsky-like region. Hilltop IGHI is attained for $n > 0$ and there we find $\Delta_{\text{max}^*} \gtrsim 0.155$, where Δ_{max^*} increases as n drops. The required tuning is not severe, mainly for $n < 0.04$ since $\Delta_{\text{max}^*} \gtrsim 20\%$. Since our models predict $r \gtrsim 0.0017$, they are testable by the forthcoming experiments, like BICEP3 [34], PRISM [35], LiteBIRD [36] and CORE [37], which are expected to measure r with an accuracy of 10^{-3} . We do not present in Table II ϕ_* values since, as inferred by Eq. (58), every ϕ_* satisfying Eq. (41a) leads to the same ratio λ/c_- . For the reasons mentioned below Eq. (56), we prefer $\phi_* \leq 1$. To achieve this, we need $c_- \gtrsim (30 - 140)$ for $K = K_1$ and $c_- \gtrsim (40 - 160)$ for $K = K_2$ or K_3 , where the variation of c_- is given as n decreases.

For $K = K_1$ we expect similar values for λ/c_- and the inflationary observables. However, r_{\pm} will differ appreciably due to the different relation between n and N – see Eq. (23f). To highlight it further, we present in Fig. 3 the r_{\pm} values, obtained by Eq. (38), as a function of n for $K = K_1$ (dashed lines) or $K = K_2$ and K_3 (solid lines). The values of the curves which are preferred by the observational data at 68% c.l. [95% c.l.] are included in the dark [light] gray segments – cf. Fig. 2. We observe that for tiny n values, r_{\pm} which is roughly $1/N$ lies close to $1/3$ for $K = K_1$ and $1/2$ for $K = K_2, K_3$. For larger $|n|$ values r_{\pm} deviates more drastically from these values.

The rather different predictions attained for low ($|n| \leq 0.1$) and large ($|n| > 0.1$) n values hint that the structure of \hat{V}_{HI}

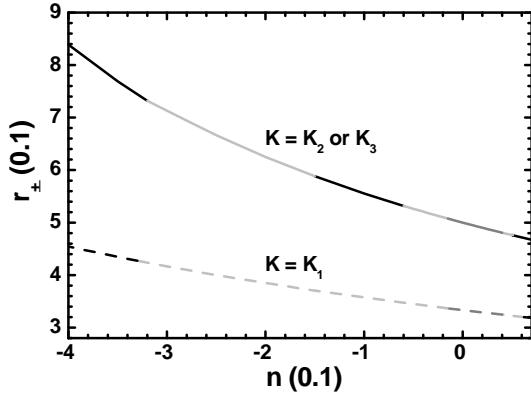


FIG. 3: Values of r_{\pm} allowed by Eq. (20) as a function of n for $K = K_1$ (dashed lines) and $K = K_2$ or K_3 (solid lines). The values which are also preferred by the observational data at 68% c.l. [95% c.l.] are included in the dark [light] gray segments.

changes drastically. To illuminate this fact we show \widehat{V}_{HI} as a function of ϕ in Fig. 4 for $K = K_2$ or K_3 , $n = 0.02$ (gray line) and $n = -0.25$ (light gray line). We take in both cases $\phi_{\star} = 1$. Therefore, the corresponding c_{-} and λ values are confined to their lowest possible values enforcing Eqs. (41a) and (41b). More specifically, we find $\lambda = 9.7 \cdot 10^{-4}$ or $5.3 \cdot 10^{-3}$ and $c_{-} = 38.1$ or 136 , with $M = 0.23$ or $M = 0.105$ for $n = 0.02$ or $n = -0.25$ respectively. The corresponding r_{\pm} values and observable quantities are listed in Table II. We see that in both cases \widehat{V}_{HI} develops a singularity at $\phi = 0$ contrary to the models of non-minimal inflation – cf. Ref. [20, 23] – where \widehat{V}_{HI} exhibits a maximum. However, for $n > 0$ and $|n| \sim 0.01$, \widehat{V}_{HI} resembles the potential of Starobinsky model with a maximum at $\phi_{\text{max}} = 1.65$. This does not affect much the inflationary evolution since we find $\Delta_{\text{max}\star} = 39\%$, and so the tuning of the initial conditions of IGHI is rather mild. On the contrary, \widehat{V}_{HI} increases monotonically and almost linearly with ϕ for $n = -0.25$. Both behaviors can be interpreted from Eq. (24) taking into account that $f_{\text{W}} \sim \phi^2$ and $f_{\text{R}} \sim \phi^2$. For $n \sim 0.01$, $\widehat{V}_{\text{HI}} \sim f_{\text{W}}^2/f_{\text{R}}^2$ becomes more or less constant, whereas for $n \simeq -0.25$, $\widehat{V}_{\text{HI}} \sim f_{\text{W}}^2/f_{\text{R}}^{2.3/4} \sim \phi^4/\phi^3 \sim \phi$. It is also remarkable that in the latter case r increases, thanks to the increase of the inflationary scale, $\widehat{V}_{\text{HI}}^{1/4}$. Similar region of parameters is recently reported in Ref. [54].

III. A POSSIBLE POST-INFLATIONARY COMPLETION

Our discussion about IGHI is certainly incomplete without at least mentioning how the transition to the radiation dominated era is realized and the observed BAU is generated. Since these goals are related to the possible decay channels of the inflaton, the connection of IGHI with some low energy theory is unavoidable. A natural, popular and well motivated framework for particle physics at the TeV scale beyond the standard model is MSSM. A possible route to such a more complete

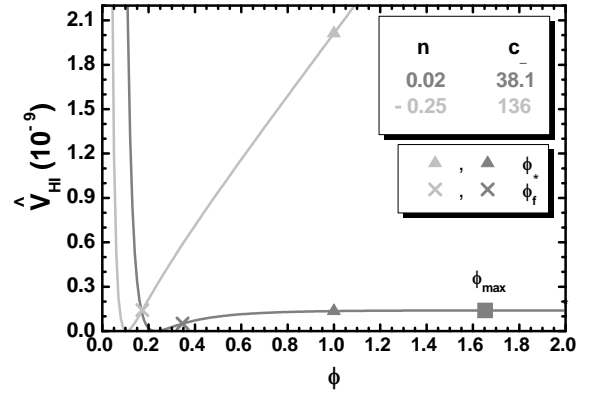


FIG. 4: The inflationary potential \widehat{V}_{HI} as a function of ϕ for $K = K_2$ or K_3 , $\phi_{\star} = 1$ and $n = 0.02$ (gray line) or $n = -0.25$ (light gray line). The values corresponding to ϕ_{\star} , ϕ_{f} and ϕ_{max} (for $n = 0.02$) are also indicated.

scenario is described in Sec. III A. Next, Sec. III B is devoted to the connection of IGHI with MSSM through the generation of the μ term. In Sec. III C, finally, we analyze the scenario of nTL exhibiting the relevant constraints and further restricting the parameters. Here and hereafter we restore units, i.e., we take $m_{\text{P}} = 2.433 \cdot 10^{18}$ GeV.

A. THE RELEVANT SET-UP

Following the post-inflationary setting of Ref. [23] we supplement the superpotential of the theory with the terms

$$W_{\text{RHN}} = \lambda_{iN^c} \bar{\Phi} N_i^{c2} + h_{Nij} N_i^c L_j H_u, \quad (67a)$$

which allows for the implementation of type I see-saw mechanism (providing masses to light neutrinos) and supports a robust baryogenesis scenario through nTL, and

$$W_{\mu} = \lambda_{\mu} S H_u H_d, \quad (67b)$$

inspired by Ref. [25], which offers a solution to one of the most tantalizing problems of MSSM, namely the generation of a μ term – for an alternative solution see Ref. [55]. Here we adopt the notation and the $B - L$ and R charges of the various superfields as displayed in Table 1 of Ref. [23]. Let us only note that L_i denotes the i -th generation $SU(2)_{\text{L}}$ doublet left-handed lepton superfields, and H_u [H_d] is the $SU(2)_{\text{L}}$ doublet Higgs superfield which couples to the up [down] quark superfields. Also, we assume that the superfields N_j^c have been rotated in the family space so that the coupling constants λ_i are real and positive. This is the so-called [3, 23] N_i^c basis, where the N_i^c masses, M_{iN^c} , are diagonal, real, and positive.

We assume that the extra fields $X^{\beta} = H_u, H_d, \tilde{N}_i^c$ have identical kinetic terms as the stabilizer field S expressed by the functions F_{lS} with $l = 1, 2, 3$ in Eqs. (9a) – (9c) – see Ref. [23]. Therefore, N_S may be renamed N_X henceforth.

TABLE III: Mass-squared spectrum of the non-inflaton sector for $K = K_{1\mathcal{R}}$ and $K_{2\mathcal{R}}$ along the path in Eqs. (22) and (68).

FIELDS	EIGEN-STATES	MASSES SQUARED		
			$K = K_{1\mathcal{R}}$	$K = K_{2\mathcal{R}}$
10 Real Scalars	$\widehat{h}_\pm, \widehat{h}_\pm^c$ $\widehat{v}_i^c, \widehat{v}_i^c$	$\widehat{m}_{h_\pm}^2$ $\widehat{m}_{i\bar{v}^c}^2$	$3\widehat{H}_{\text{HI}}^2 c_{\mathcal{R}} (\phi^2/2N \pm 2\lambda_\mu/\lambda)$ $3\widehat{H}_{\text{HI}}^2 c_{\mathcal{R}} (\phi^2/2N + 8\lambda_{iN^c}^2/\lambda^2)$	$3\widehat{H}_{\text{HI}}^2 (1 + 1/N_X \pm 4\lambda_\mu/\lambda\phi^2)$ $3\widehat{H}_{\text{HI}}^2 (1 + 1/N_X + 16\lambda_{iN^c}^2/\lambda^2\phi^2)$
3 Weyl Spinors	\widehat{N}_i^c	$\widehat{m}_{iN^c}^2$	$48\widehat{H}_{\text{HI}}^2 \lambda_{iN^c}^2/\lambda^2\phi^2$	

TABLE IV: The same as Table III but for $K = K_1, K_3$ and K_3 .

FIELDS	EIGEN-STATES	MASSES SQUARED			
			$K = K_1$	$K = K_2$	$K = K_3$
10 Real Scalars	$\widehat{h}_\pm, \widehat{h}_\pm^c$ $\widehat{v}_i^c, \widehat{v}_i^c$	$\widehat{m}_{h_\pm}^2$ $\widehat{m}_{i\bar{v}^c}^2$	$3\widehat{H}_{\text{HI}}^2 (1 + f_W/N \pm 4\lambda_\mu c_+^2 \phi^2/\lambda f_W)$ $3\widehat{H}_{\text{HI}}^2 ((1 + f_W/N)/c_+ \phi^2 + 16\lambda_{iN^c}^2 c_+^2 \phi^2/\lambda^2 f_W^2)$	$3\widehat{H}_{\text{HI}}^2 (1 + 1/N_X \pm 4\lambda_\mu c_+/\lambda f_W)$ $3\widehat{H}_{\text{HI}}^2 (1 + 1/N_X + 16\lambda_{iN^c}^2 c_+^2 \phi^2/\lambda^2 f_W^2)$	
3 Weyl Spinors	\widehat{N}_i^c	$m_{iN^c}^2$	$48\lambda_{iN^c}^2 c_+^2 \phi^2 \widehat{H}_{\text{HI}}^2/\lambda^2 f_W^2$		

The inflationary trajectory in Eq. (22) has to be supplemented by the conditions

$$H_u = H_d = \widetilde{N}_i^c = 0, \quad (68)$$

and the stability of this path has to be checked, parameterizing the complex fields above as we do for S in Eq. (21). The relevant masses squared are listed in Table III for $K = K_{1\mathcal{R}}$ and $K_{2\mathcal{R}}$ and Table IV for $K = K_1, K_2$ and K_3 , where we see that $\widehat{m}_{i\bar{v}^c}^2 > 0$ and $\widehat{m}_{h_\pm}^2 > 0$ for every ϕ . On the other hand, the positivity of the eigenvalues $\widehat{m}_{h_\pm}^2$ associated with the eigenstates \widehat{h}_+ and \widehat{h}_- , where

$$\widehat{h}_\pm = (\widehat{h}_u \pm \widehat{h}_d)/\sqrt{2} \quad \text{and} \quad \widehat{h}_\pm^c = (\widehat{h}_u \pm \widehat{h}_d)/\sqrt{2}, \quad (69)$$

with the hatted fields being defined as \widehat{h} and \widehat{h}^c in Eq. (33b), requires the establishment of the inequalities

$$\lambda_\mu \lesssim \lambda\phi^2/4N \quad \text{for } K = K_{1\mathcal{R}}, \quad (70a)$$

$$\lambda_\mu \lesssim \lambda\phi^2(1 + 1/N_X)/4 \quad \text{for } K = K_{2\mathcal{R}}, \quad (70b)$$

$$\lambda_\mu \lesssim \lambda f_W(1 + f_W/N)/4\lambda_\mu c_+^2 \phi^2 \quad \text{for } K = K_1, \quad (70c)$$

$$\lambda_\mu \lesssim \lambda f_W(1 + 1/N_X)/4c_+ \quad \text{for } K = K_2, K_3. \quad (70d)$$

In all cases, the inequalities are fulfilled for $\lambda_\mu \lesssim 2 \cdot 10^{-5}$. Similar numbers are obtained in Ref. [3, 23]. We do not consider such a condition on λ_μ as unnatural, given that the Yukawa coupling constant h_{1U} , which provides masses to the up-type quarks, is of the same order of magnitude too at a high scale – cf. Ref. [56]. Note that the hierarchy in Eqs. (70a) – (70d) between λ_μ and λ differs from that imposed in the models [25] of F-term hybrid inflation, where S plays the role of inflaton and $\Phi, \bar{\Phi}, H_u$ and H_d are confined at zero. Indeed, in that case we demand [25] $\lambda_\mu > \lambda$ so that the tachyonic instability in the $\Phi - \bar{\Phi}$ direction occurs first, and the $\Phi - \bar{\Phi}$ system start evolving towards its v.e.v, whereas H_u and H_d continue to be confined to zero. In our case, though, the inflaton is included in the $\bar{\Phi} - \Phi$ system while S and the $H_u - H_d$

system are safely stabilized at the origin both during and after IGHI. Therefore, ϕ settles in its vacuum and S, H_u and H_d take their non-vanishing electroweak scale v.e.vs afterwards.

B. A SOLUTION TO THE μ PROBLEM OF MSSM

A byproduct of the R symmetry associated with our models is that it assists us to understand the origin of the μ term of MSSM – see Sec. III B 1 – connecting thereby the high with the low energy phenomenology as described in Sec. III B 2.

1. Generating the μ Parameter

Working along the lines of Sec. II A 2 we can verify that the presence of the terms in Eqs. (67a) and (67b) leave the v.e.vs in Eq. (19) unaltered whereas those of X^β are found to be

$$\langle H_u \rangle = \langle H_d \rangle = \langle \widetilde{N}_i^c \rangle = 0. \quad (71)$$

On the other hand, the contributions from the soft SUSY breaking terms, although negligible during IGHI – since these are expected to be much smaller than ϕ –, may slightly shift [3, 23, 25] $\langle S \rangle$ from zero in Eq. (19). Indeed, the relevant potential terms are

$$V_{\text{soft}} = (\lambda A_\lambda S \bar{\Phi} \Phi - a_S S \lambda M^2/4 + \text{h.c.}) + m_\gamma^2 |X^\gamma|^2, \quad (72)$$

where $X^\gamma = \Phi, \bar{\Phi}, S, H_u, H_d, \widetilde{N}_i^c$, and m_γ, A_λ and a_S are soft SUSY breaking mass parameters of the order of TeV. The emergence of these terms depend on the mechanism of SUSY breaking which is not specified here. We restrict ourselves to the assumption that this extra sector of the theory may be included in the present set-up without disturbing the status of inflation – cf. Ref. [57]. Confining $\Phi, \bar{\Phi}, H_u, H_d$ and N_i^c in their v.e.vs in Eqs. (19) and (71), \widehat{V} in Eq. (10b) reduces

again to V_{eff} in Eq. (15a) with vanishing terms represented by ellipsis since $\langle W_{\text{HI}} \rangle = 0$. We then rotate S to the real axis by an appropriate R -transformation and choose conveniently the phases of A_λ and a_S so as the total low-energy potential

$$V_{\text{tot}} = V_{\text{eff}} + V_{\text{soft}} \quad (73)$$

to be minimized. Since the form of V_{eff} depends on the adopted K , we single out the cases:

(a) $K = K_1, K_2$ and K_3 . Focusing on $K = K_2$ or K_3 we obtain

$$\langle V_{\text{tot}}(S) \rangle \simeq \frac{\lambda^2 S^2}{2(\det M_\pm)} (c_- M^2 - N m_{\text{P}}^2) - \lambda a_{3/2} m_{3/2} M^2 S, \quad (74a)$$

where the first term in the r.h.s originates from the second line of Eq. (18) for $e^{\tilde{K}+/m_{\text{P}}^2} \simeq 1$, and Φ and $\bar{\Phi}$ equal to their v.e.vs in Eq. (19). Also, we take into account that $m_S \ll M$, and we set

$$|A_\lambda| + |a_S| = 2a_{3/2} m_{3/2}, \quad (74b)$$

where $m_{3/2}$ is the \tilde{G} mass and $a_{3/2} > 0$ a parameter of order unity which parameterizes our ignorance of the dependence of $|A_\lambda|$ and $|a_S|$ on $m_{3/2}$. The minimization condition for the total potential in Eq. (74a) w.r.t S leads to a non vanishing $\langle S \rangle$ as follows

$$\frac{d}{dS} \langle V_{\text{tot}}(S) \rangle = 0 \Rightarrow \langle S \rangle \simeq a_{3/2} m_{3/2} c_- (1 + N r_\pm) / \lambda, \quad (74c)$$

since from Eqs. (17c), (19) and (20) we infer

$$\langle \det M_\pm \rangle = c_-^2 - N^2 c_+^2 = c_-^2 (1 + N r_\pm) (1 - N r_\pm). \quad (74d)$$

At this S value, $\langle V_{\text{tot}}(S) \rangle$ develops a minimum since

$$\frac{d^2}{dS^2} \langle V_{\text{tot}}(S) \rangle = \lambda^2 / c_+ (c_- + N c_+) > 0. \quad (74e)$$

For $K = K_1$ Eq. (74c) can be obtained again by doing an expansion of the relevant expressions in powers $1/m_{\text{P}}$.

The μ term generated from Eq. (67b) exhibits the mixing parameter

$$\mu = \lambda_\mu \langle S \rangle \simeq \lambda_\mu a_{3/2} m_{3/2} c_- (1 + N r_\pm) / \lambda. \quad (75a)$$

Comparing this result with the corresponding one in Ref. [23], we deduce a crucial difference regarding the sign of the expression in the parenthesis which originates from the terms in the second line of Eq. (18). With the aid of Eq. (58) we may eliminate c_- and λ from the above result which then reads

$$\mu \simeq 1.2 \cdot 10^2 \lambda_\mu \frac{a_{3/2} m_{3/2} (1 + N r_\pm) (f_{\mathcal{R}^*} - 1)^2}{r_\pm^{3/2} f_{\mathcal{R}^*}^{n+1/2} (n(1 - f_{\mathcal{R}^*}) + 1)}, \quad (75b)$$

where Eq. (41b) is employed to obtain the numerical prefactor. Taking into account Eqs. (38) and (54), we infer that the resulting μ depends only on n and not on λ, c_- and r_\pm – cf.

Ref. [23, 25]. For the λ_μ values allowed by Eqs. (70c) and (70d), any $|\mu|$ value is accessible with a mild hierarchy between $m_{3/2}$ and μ – from Table IV we see that both signs of λ_μ (and so μ) are possible without altering the stability analysis of the inflationary system. To understand this, let us first remark that Eq. (20) implies $r_\pm \simeq 1/N$ and $f_{\mathcal{R}^*}$ varies from about 12 to 68 [15 to 119] for $K = K_1$ [$K = K_2$ and K_3], as n varies in the allowed ranges of Eqs. (64) – (66). A rough estimation gives $\mu \sim 10^2 \lambda_\mu f_{\mathcal{R}^*}^{3/2} = 10^{-1.5} m_{3/2}$ and so we expect that μ is about one order of magnitude less than $m_{3/2}$.

(b) $K = K_{1\mathcal{R}}$ and $K_{2\mathcal{R}}$. In this case, V_{tot} in Eq. (73) with all the fields except S equal to their v.e.vs in Eqs. (19) and (71) is written as

$$\langle V_{\text{tot}}(S) \rangle = \frac{\lambda^2 m_{\text{P}}^2 S^2}{c_{\mathcal{R}} (N c_{\mathcal{R}} - 1)} - \lambda a_{3/2} m_{3/2} M^2 S. \quad (76a)$$

The minimization of $\langle V_{\text{tot}}(S) \rangle$ w.r.t S leads to a new non vanishing $\langle S \rangle$,

$$\langle S \rangle \simeq N a_{3/2} m_{3/2} c_{\mathcal{R}} / \lambda, \quad (76b)$$

where M is replaced by Eq. (20). Therefore, the μ parameter involved in Eq. (67b) is

$$\mu = \lambda_\mu \langle S \rangle = N \lambda_\mu a_{3/2} m_{3/2} c_{\mathcal{R}} / \lambda. \quad (76c)$$

This still depends only n thanks to the condition in Eq. (48) which fixes $\lambda/c_{\mathcal{R}}$ as a function of n – see Eq. (47).

To highlight further the conclusions above, we can employ Eq. (75a) to derive the $m_{3/2}$ values required so as to obtain a specific μ value. Given that Eq. (75a) depends on n , which crucially influences n_s and r , we expect that the required $m_{3/2}$ is a function of n_s and r as depicted in Fig. 5-(a) and Fig. 5-(b) respectively. We take $\lambda_\mu = 10^{-6}$, in accordance with Eqs. (70c) and (70d), $a_{3/2} = 1$, $K = K_2$ or K_3 with $N_X = 2$ and $\mu = 0.5$ TeV (dot-dashed line), $\mu = 1$ TeV (solid line), or $\mu = 2$ TeV (dashed line). Varying n in the allowed range indicated in Fig. 2-(a) we obtain the variation of $m_{3/2}$ solving Eq. (75a) w.r.t $m_{3/2}$. The values of the curves which are preferred by the observational data at 68% c.l. [95% c.l.] are included in the dark [light] gray segments – cf. Fig. 2. We see that $m_{3/2}$ increases with μ and its lowest value $m_{3/2} \simeq 4$ TeV is obtained for $\mu = 0.5$ TeV. As we anticipated above, $m_{3/2}$ is almost one order of magnitude larger than the corresponding μ . Moreover, for fixed μ , each curve develops a maximum at $n \simeq -0.15$, which coincides with the right corner of the curve in Fig. 2. This behavior deviates a lot from the one found in Ref. [23] and comes from the different sign in the parenthesis of Eq. (75a).

2. Connection with the Parameters of CMSSM

The SUSY breaking effects, considered in Eq. (72), explicitly break $U(1)_R$ to a subgroup, \mathbb{Z}_2^R which can be identified

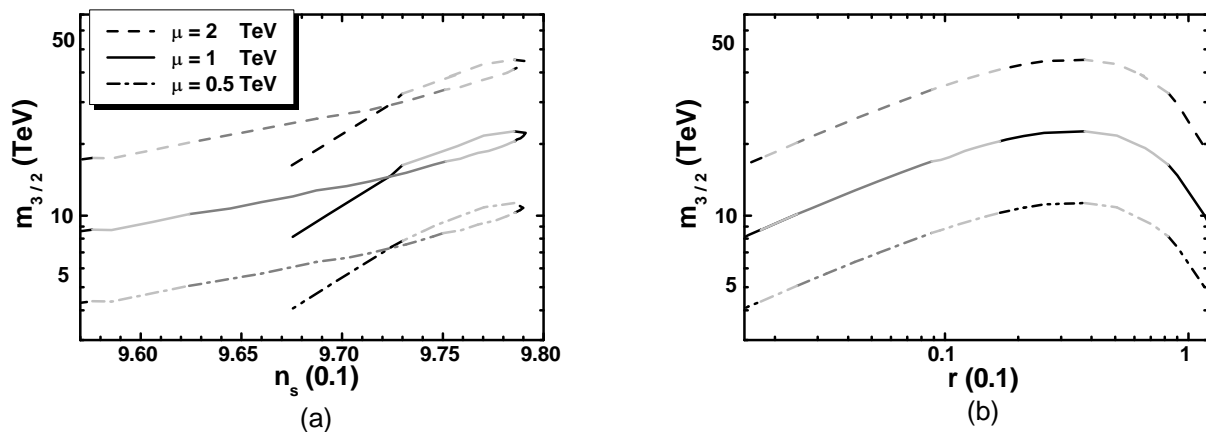


FIG. 5: The gravitino mass $m_{3/2}$ versus n_s (a) and r (b) for $\lambda_\mu = 10^{-6}$, $a_{3/2} = 1$, $K = K_2$ or K_3 with $N_X = 2$ and $\mu = 0.5$ TeV (dot-dashed line), $\mu = 1$ TeV (solid line), or $\mu = 2$ TeV (dashed line). The color coding is as in Fig. 3.

TABLE V: The required λ_μ values rendering our models compatible with the best-fit points of the CMSSM as found in Ref. [58] with the assumptions in Eq. (77).

CMSSM REGION:	A/H FUNNEL	COANNIHILATION		
		$\tilde{\tau}_1 - \chi$	$\tilde{t}_1 - \chi$	$\tilde{\chi}_1^\pm - \chi$
$ A_0 $ (TeV)	9.924	1.227	9.965	9.2061
m_0 (TeV)	9.136	1.476	4.269	9.000
$ \mu $ (TeV)	1.409	2.62	4.073	0.983
$a_{3/2}$	1.086	0.831	2.33	1.023
$\lambda_\mu(10^{-6})$ for $K = K_{1\mathcal{R}}$				
$n = 0$	0.963	14.48	2.91	0.723
$\lambda_\mu(10^{-6})$ for $K = K_{2\mathcal{R}}$				
$n = 0$	1.184	17.81	3.41	0.89
$\lambda_\mu(10^{-6})$ for $K = K_1$				
$n = 0.02$	1.409	21.19	4.063	1.059
$n = -0.25$	1.87	28.11	5.39	1.405
$\lambda_\mu(10^{-6})$ for $K = K_2$ and K_3				
$n = 0.02$	1.814	27.28	5.23	1.363
$n = -0.25$	2.784	41.86	8.025	2.092

with a matter parity. Under this discrete symmetry all the matter (quark and lepton) superfields change sign – see Table 1 of Ref. [23]. Since S has the R symmetry of the total superpotential of the theory, $\langle S \rangle$ in Eq. (74c) also breaks spontaneously $U(1)_R$ to \mathbb{Z}_2^R . Thanks to this fact, \mathbb{Z}_2^R remains unbroken and so no disastrous domain walls are formed. Combining \mathbb{Z}_2^R with the \mathbb{Z}_2^f fermion parity, under which all fermions change sign, yields the well-known R -parity. This residual symmetry prevents rapid proton decay and guarantees the stability of the *lightest SUSY particle* (LSP), providing thereby a well-motivated *cold dark matter* (CDM) candidate.

The candidacy of LSP may be successful, if it generates the correct CDM abundance [53] within a concrete low energy framework, which in our case is the MSSM or one of its vari-

ants – for an alternative approach within high-scale SUSY see Ref. [59]. Here, we adopt the *Constrained MSSM* (CMSSM) which is the most restrictive, predictive and well-motivated version of MSSM, which allows the lightest neutralino to play the role of LSP in a sizable portion of the parametric space. This is based on the free parameters

$$\text{sign}\mu, \quad \tan\beta = \langle H_u \rangle / \langle H_d \rangle, \quad M_{1/2}, \quad m_0, \quad \text{and} \quad A_0,$$

where $\text{sign}\mu$ is the sign of μ , and the three last mass parameters denote the common gaugino mass, scalar mass and trilinear coupling constant, respectively, defined (normally) at M_{GUT} . The parameter $|\mu|$ is not free, since it is computed at low scale by enforcing the conditions for the electroweak symmetry breaking. The values of these parameters can be tightly restricted imposing a number of cosmological constraints from which the consistency of LSP relic density with observations plays a central role. Some updated results are recently presented in Ref. [58], where we can also find the best-fit values of $|A_0|$, m_0 and $|\mu|$ listed in the first four lines of Table V. We see that there are four allowed regions characterized by the mechanism applied for accommodating an acceptable CDM abundance.

Taking advantage of this investigation, we can check whether the μ and $m_{3/2}$ values satisfying Eq. (75a) are consistent with these values. Selecting some representative n values and adopting the identifications

$$m_0 = m_{3/2} \quad \text{and} \quad |A_\lambda| = |a_S| = |A_0|, \quad (77)$$

we can first derive $a_{3/2}$ from Eq. (74b) and then the λ_μ values from Eqs. (75a) – (76c), which yield the phenomenologically desired $|\mu|$ shown in the third line of Table V. Here we assume that renormalization effects in the derivation of μ are negligible. The outputs of our computation are assembled in the last ten lines of Table V. As inputs, we take $n = 0.0$ for $K = K_{1\mathcal{R}}$ and $K_{2\mathcal{R}}$ $n = 0.02$ and -0.25 for $K = K_1, K_2$ and K_3 . These are central values in the regions compatible with the inflationary observations as found in Sec. IIC 3. The λ_μ values for $K = K_{1\mathcal{R}}$ and $K_{2\mathcal{R}}$ are lower than those obtained for $K = K_1, K_2$ and K_3 , larger than those found in Ref. [23],

and similar to those in Ref. [3] especially for $K = K_{1\mathcal{R}}$. On the other hand, the λ_μ values found for $K = K_1, K_2$ and K_3 are larger compared to those found in Refs. [3, 23].

From the outputs we infer that the required λ_μ values are comfortably compatible with Eqs. (70a) – (70d) for $N_X = 2$, in all cases besides the one corresponding to the $\tilde{\tau}_1 - \chi$ coannihilation region. In that case, m_0 is lower than $|\mu|$ and so marginally large λ_μ values are required. In the cases where numbers are written in italics, we obtain instability along the inflationary path for $K = K_{1\mathcal{R}}$ and K_1 , whereas for $K = K_{2\mathcal{R}}, K_2$ and K_3 we need $0 \leq N_X \leq 1$ to avoid this effect. In sharp contrast to the model of Ref. [23], only the A/H funnel and $\tilde{\chi}_1^\pm - \chi$ coannihilation regions can be consistent with the \tilde{G} limit on T_{rh} – see Sec. III C 2. Indeed, $m_{3/2} \gtrsim 9$ TeV become cosmologically safe under the assumption of an unstable \tilde{G} , for the T_{rh} values necessitated for satisfactory leptogenesis – see Sec. III C 3.

C. NON-THERMAL LEPTOGENESIS

Our next task is to specify how our inflationary scenario makes a transition to the radiation dominated era – see Sec. III C 1 – and offers an explanation of the observed BAU consistent with the \tilde{G} constraint and the low energy neutrino data – see Sec. III C 2. Our results are summarized in Sec. III C 3.

1. Inflaton Mass and Decay

When IGHI is over, the inflaton continues to roll down towards the SUSY vacuum, Eq. (19). Soon after, it settles into a phase of damped oscillations around the minimum of \hat{V}_{HI} . The (canonically normalized) inflaton,

$$\widehat{\delta\phi} = \langle J \rangle \delta\phi \quad \text{with} \quad \delta\phi = \phi - M, \quad (78)$$

and

$$\langle J \rangle = \begin{cases} \sqrt{N c_{\mathcal{R}}} & \text{for } K = K_{1\mathcal{R}} \text{ and } K_{2\mathcal{R}}, \\ \sqrt{c_- (1 + N r_\pm)} & \text{for } K = K_1, K_2 \text{ and } K_3, \end{cases} \quad (79)$$

acquires mass, at the SUSY vacuum in Eq. (19), which is given by

$$\frac{\widehat{m}_{\delta\phi}}{\lambda m_{\text{P}}} = \begin{cases} \sqrt{c_{\mathcal{R}} (N c_{\mathcal{R}} - 1)} & \text{for } K = K_{1\mathcal{R}} \text{ and } K_{2\mathcal{R}}, \\ c_- \sqrt{2(1 + N r_\pm)} & \text{for } K = K_1, K_2 \text{ and } K_3. \end{cases} \quad (80)$$

From the last expression we can infer that $\widehat{m}_{\delta\phi}$ remains constant for fixed n since $\lambda/c_{\mathcal{R}}$ [λ/c_-] is fixed too – see Eqs. (48) and (58). More specifically, for the allowed range of n in Eqs. (61a) and (61b) we obtain

$$2. \lesssim \widehat{m}_{\delta\phi}/10^{13} \text{ GeV} \lesssim 3.9 \quad \text{for } K = K_{1\mathcal{R}}, \quad (81a)$$

$$2.1 \lesssim \widehat{m}_{\delta\phi}/10^{13} \text{ GeV} \lesssim 4.5 \quad \text{for } K = K_{2\mathcal{R}}, \quad (81b)$$

with the value $\widehat{m}_{\delta\phi} = 2.8 \cdot 10^{13}$ GeV corresponding to $n = 0$. Furthermore, for $K = K_1$ and the allowed range of n in Eq. (64) we obtain

$$2.9 \lesssim \widehat{m}_{\delta\phi}/10^{13} \text{ GeV} \lesssim 5. \quad (82a)$$

For $K = K_2$ and K_3 , in the allowed ranges of Eqs. (65) and (66), we obtain

$$3.1 \lesssim \widehat{m}_{\delta\phi}/10^{13} \text{ GeV} \lesssim 6.9; \quad (82b)$$

$$4.1 \lesssim \widehat{m}_{\delta\phi}/10^{13} \text{ GeV} \lesssim 7.2. \quad (82c)$$

We remark that $\widehat{m}_{\delta\phi}$ is somewhat affected by the choice of K 's in Eqs. (6a) – (6c). For $n = 0$, $\widehat{m}_{\delta\phi} = 4.7 \cdot 10^{13}$ GeV for $K = K_1$, and $\widehat{m}_{\delta\phi} = 5.2 \cdot 10^{13}$ GeV for $K = K_2$ and K_3 , which are both somewhat larger than the value obtained within Starobinsky inflation [3, 6]. On the other hand, these values are close to the maximal ones found in Ref. [23], since here r_\pm approaches its maximal value.

The inflaton can decay [60] perturbatively into:

(a) A pair of N_i^c with Majorana masses $M_{iN^c} = \lambda_{iN^c} M$ with the decay width

$$\widehat{\Gamma}_{\delta\phi \rightarrow N_i^c N_i^c} = \frac{g_{iN^c}^2 \widehat{m}_{\delta\phi}}{16\pi} \left(1 - \frac{4M_{iN^c}^2}{\widehat{m}_{\delta\phi}^2} \right)^{3/2}, \quad (83a)$$

where the relevant coupling constant

$$g_{iN^c} = (N - 1) \frac{\lambda_{iN^c}}{\langle J \rangle} \quad (83b)$$

arises from the lagrangian term

$$\begin{aligned} \mathcal{L}_{\widehat{\delta\phi} \rightarrow N_i^c N_i^c} &= -\frac{1}{2} e^{K/2m_{\text{P}}^2} W_{\text{RH}, N_i^c N_i^c} N_i^c N_i^c + \text{h.c.} \\ &= g_{iN^c} \widehat{\delta\phi} N_i^c N_i^c + \text{h.c.} \end{aligned} \quad (83c)$$

This decay channel activates the mechanism of nTL, as sketched in Sec. III C 2.

(b) Higgses H_u and H_d with the decay width

$$\widehat{\Gamma}_{\delta\phi \rightarrow H_u H_d} = \frac{2}{8\pi} g_H^2 \widehat{m}_{\delta\phi} \quad \text{where} \quad g_H = \frac{\lambda_\mu}{\sqrt{2}} \quad (84a)$$

arises from the lagrangian term

$$\begin{aligned} \mathcal{L}_{\widehat{\delta\phi} \rightarrow H_u H_d} &= -e^{K/m_{\text{P}}^2} K^{SS^*} |W_{\mu,S}|^2 \\ &= -g_H \widehat{m}_{\delta\phi} \widehat{\delta\phi} (H_u^* H_d^* + \text{h.c.}) + \dots \end{aligned} \quad (84b)$$

Thanks to the upper bounds on λ_μ from Eqs. (70c) and (70d), g_H turns out to be comparable with g_{iN^c} .

(c) MSSM (s)-particles XYZ with the following c_+ -dependent 3-body decay width

$$\widehat{\Gamma}_{\delta\phi \rightarrow XYZ} = g_y^2 \frac{n_f}{512\pi^3} \frac{\widehat{m}_{\delta\phi}^3}{m_{\text{P}}^2}, \quad (85a)$$

where for the third generation we take $y \simeq (0.4 - 0.6)$, computed at the $\widehat{m}_{\delta\phi}$ scale, and $n_f = 14$ for $\widehat{m}_{\delta\phi} < M_{3N^c}$. Also,

$$g_y = y_3 \cdot \begin{cases} \sqrt{(Nc_{\mathcal{R}} - 1)/2c_{\mathcal{R}}} & \text{for } K = K_{1\mathcal{R}} \text{ and } K_{2\mathcal{R}}, \\ N\sqrt{r_{\pm}/(1 + Nr_{\pm})} & \text{for } K = K_1, K_2 \text{ and } K_3 \end{cases} \quad (85b)$$

and $y_3 = h_{t,b,\tau}(\widehat{m}_{\delta\phi}) \simeq 0.5$. Since $r_{\pm} \simeq 1/N$ we can easily infer that g_y above is enhanced compared to the corresponding one in Ref. [23] where $r_{\pm} \simeq 0.01$, and an additional suppression through a ratio M/m_{P} exists. We therefore expect that $\widehat{\Gamma}_{\delta\phi \rightarrow XYZ}$ contributes sizably to the total decay width of $\widehat{\delta\phi}$. Each individual decay width arises from the langrangian terms

$$\begin{aligned} \mathcal{L}_{\widehat{\delta\phi} \rightarrow X\psi_Y\psi_Z} &= -\frac{1}{2} e^{K/2m_{\text{P}}^2} (W_{y,YZ}\psi_Y\psi_Z) + \text{h.c.} \\ &= -g_y \frac{\widehat{\delta\phi}}{m_{\text{P}}} (X\psi_Y\psi_Z) + \text{h.c.}, \end{aligned} \quad (85c)$$

where $W_y = yXYZ$ is a typical trilinear superpotential term of MSSM with y a Yukawa coupling constant, and ψ_X, ψ_Y and ψ_Z are the chiral fermions associated with the superfields X, Y and Z whose scalar components are denoted with the superfield symbols.

The resulting reheat temperature is given by [61]

$$T_{\text{rh}} = (72/5\pi^2 g_*)^{1/4} \widehat{\Gamma}_{\delta\phi}^{1/2} m_{\text{P}}^{1/2}, \quad (86a)$$

with the total decay width of $\widehat{\delta\phi}$ being

$$\widehat{\Gamma}_{\delta\phi} = \widehat{\Gamma}_{\delta\phi \rightarrow N_i^c N_i^c} + \widehat{\Gamma}_{\delta\phi \rightarrow H_u H_d} + \widehat{\Gamma}_{\delta\phi \rightarrow XYZ}. \quad (86b)$$

Here, $g_* = 228.75$ counts the MSSM effective number of relativistic degrees of freedom at temperature T_{rh} . Let us clarify here that in our models there is no decay of a scalaron as in the original (non-SUSY) [2] Starobinsky inflation and some [62] of its SUGRA realizations; thus, T_{rh} in our case is slightly lower than that obtained there.

2. Lepton-Number and Gravitino Abundances

For $T_{\text{rh}} < M_{iN^c}$, the out-of-equilibrium decay of ν_i^c generates a lepton-number asymmetry (per ν_i^c decay), ε_i – see, e.g., Ref. [38, 39]. The resulting ε_i is partially converted through sphaleron effects into a yield of the observed BAU [23, 38, 39],

$$Y_B = -0.35 \cdot 2 \cdot \frac{5}{4} \frac{T_{\text{rh}}}{\widehat{m}_{\delta\phi}} \sum_i \frac{\widehat{\Gamma}_{\delta\phi \rightarrow N_i^c N_i^c}}{\widehat{\Gamma}_{\delta\phi}} \varepsilon_i, \quad (87)$$

which has to reproduce the observational result [53]

$$Y_B = (8.64_{-0.16}^{+0.15}) \cdot 10^{-11}. \quad (88)$$

The validity of Eq. (87) requires that the $\widehat{\delta\phi}$ decay into a pair of N_i^c 's is kinematically allowed for at least one species of the N_i^c 's and also that there is no erasure of the produced Y_L due to N_1^c mediated inverse decays and $\Delta L = 1$ scatterings [64]. These prerequisites are ensured if we impose

$$(a) \widehat{m}_{\delta\phi} \geq 2M_{1N^c} \text{ and } (b) M_{1N^c} \gtrsim 10T_{\text{rh}}. \quad (89)$$

The quantity ε_i can be expressed in terms of the Dirac masses of ν_i, m_{iD} , arising from the second term of Eq. (67a) – see Ref. [23]. Moreover, employing the seesaw formula we can then obtain the light-neutrino mass matrix m_ν in terms of m_{iD} and M_{iN^c} . As a consequence, nTL can be nicely linked to low energy neutrino data. We take as inputs the best-fit values [44] – see also Ref. [45] – of the neutrino mass-squared differences, $\Delta m_{21}^2 = 7.6 \cdot 10^{-5} \text{ eV}^2$ and $\Delta m_{31}^2 = (2.48 [-2.38]) \cdot 10^{-3} \text{ eV}^2$, of the mixing angles, $\sin^2 \theta_{12} = 0.323$, $\sin^2 \theta_{13} = 0.0226$ [$\sin^2 \theta_{13} = 0.029$] and $\sin^2 \theta_{23} = 0.567$ [$\sin^2 \theta_{23} = 0.573$], and of the CP-violating Dirac phase $\delta = 1.41\pi$ [$\delta = 1.48\pi$] for *normal [inverted] ordered (NO [IO]) neutrino masses, $m_{i\nu}$'s*. The sum of $m_{i\nu}$'s is bounded from above by the data [53],

$$\sum_i m_{i\nu} \leq 0.23 \text{ eV} \quad (90)$$

at 95% c.l. This is more restrictive than the 90% c.l. upper bound arising from the effective electron neutrino mass in β -decay [65]:

$$m_\beta \leq (0.061 - 0.165) \text{ eV}, \quad (91)$$

where the range accounts for nuclear matrix element uncertainties.

The required T_{rh} in Eq. (87) must be compatible with constraints on the \widetilde{G} abundance, $Y_{3/2}$, at the onset of *nucleosynthesis (BBN)*, which are [42] given approximately by

$$Y_{3/2} \lesssim \begin{cases} 10^{-14} \\ 10^{-13} \\ 10^{-12} \end{cases} \text{ for } m_{3/2} \simeq \begin{cases} 0.69 \text{ TeV}, \\ 10.6 \text{ TeV}, \\ 13.5 \text{ TeV}. \end{cases} \quad (92)$$

Here we consider the conservative case where \widetilde{G} decays with a tiny hadronic branching ratio. The bounds above can be somehow relaxed in the case of a stable \widetilde{G} – see e.g. Ref. [28].

In our models $Y_{3/2}$ is estimated to be [41, 42]:

$$Y_{3/2} \simeq 1.9 \cdot 10^{-22} T_{\text{rh}}/\text{GeV}, \quad (93)$$

where we take into account only thermal production of \widetilde{G} , and assume that \widetilde{G} is much heavier than the MSSM gauginos. Non-thermal contributions to $Y_{3/2}$ [60] are also possible but strongly dependent on the mechanism of soft SUSY breaking. Moreover, no precise computation of this contribution exists within IGH1 adopting the simplest Polonyi model of SUSY breaking [43]. It is notable, though, that the non-thermal contribution to $Y_{3/2}$ in models with stabilizer field, as in our case, is significantly suppressed compared to the thermal one.

3. Results

It is worthwhile to test the applicability of the framework above in the case of IGH. Namely, following a bottom-up approach detailed in Ref. [23], we find the M_{iN^c} 's by using as inputs the m_{iD} 's, a reference mass of the ν_i 's – $m_{1\nu}$ for NO $m_{i\nu}$'s, or $m_{3\nu}$ for IO $m_{i\nu}$'s –, the two Majorana phases φ_1 and φ_2 of the PMNS matrix, and the best-fit values, mentioned in Sec. III C 2, for the low energy parameters of neutrino physics – note that there are no experimental constraints on φ_1 and φ_2 up to now. In our numerical code we also estimate, following Ref. [63], the renormalization group evolved values of the latter parameters at the scale of nTL, $\Lambda_L = \hat{m}_{\delta\phi}$, by considering the MSSM with $\tan\beta \simeq 50$ as an effective theory between Λ_L and the soft SUSY breaking scale, $M_{\text{SUSY}} = 1.5$ TeV. We evaluate the M_{iN^c} 's at Λ_L , and we neglect any possible running of the m_{iD} 's and M_{iN^c} 's. Therefore, we present their values at Λ_L .

We start the exposition of our results arranging in Table VI for $K = K_2$ or K_3 and VII for $K = K_{2\mathcal{R}}$ some representative values of the parameters which yield Y_B and $Y_{3/2}$ compatible with Eqs. (88) and (92), respectively. Throughout our computation we take $\lambda_\mu = 10^{-6}$, in accordance with Eqs. (70c) and (70d), and $y = 0.5$, which is a typical value encountered [56] in various MSSM settings with large $\tan\beta$. Also, we select $n = 0.02$ in Table VI and $n = 0$ in Table VII. These values yield n_s and r in the ‘‘sweet’’ spot of the present data – see Figs. 2 and 1. We obtain $M = 2.85 \cdot 10^{16}$ GeV and $\hat{m}_{\delta\phi} = 2.8 \cdot 10^{13}$ GeV for $K = K_{1\mathcal{R}}$ or $K_{2\mathcal{R}}$, $M = 6.1 \cdot 10^{17}$ GeV and $\hat{m}_{\delta\phi} = 4.2 \cdot 10^{13}$ GeV for $K = K_1$, or $M = 5.6 \cdot 10^{15}$ GeV and $\hat{m}_{\delta\phi} = 4.4 \cdot 10^{13}$ GeV for $K = K_2$ or K_3 . Although the uncertainties from the choice of K 's are negligible as regards the quantities above, the decay widths in Sec. III C 1 depend on N (and r_\pm) which take slightly different values for $K = K_{1\mathcal{R}}$ or K_1 and $K = K_{2\mathcal{R}}$, K_2 or K_3 – see e.g. Fig. 3 – discriminating somehow the various choices. For this reason, we clarify that we adopt $K = K_{2\mathcal{R}}$ in Table VII and $K = K_2$ or K_3 in Table VI. Had we employed $K = K_{1\mathcal{R}}$ or K_1 , we would have obtained almost two times larger Y_B 's with the same values of the free parameters. Therefore a mild readjustment is needed.

In both Tables we consider NO (cases A and B), almost degenerate (cases C, D and E) and IO (cases F and G) $m_{i\nu}$'s. In all cases Eq. (90) is safely met – the case D saturates it – whereas Eq. (91) is comfortably satisfied. The gauge group adopted here, G_{B-L} , does not predict any relation between the Yukawa couplings constants h_{iN} entering the second term of Eq. (67a) and the other Yukawa couplings in the MSSM. As a consequence, the m_{iD} 's are free parameters. However, for the sake of comparison, for cases A – F, we take $m_{3D} = m_t(\Lambda_L) \simeq 100$ GeV, where m_t denotes the mass of the top quark. Similar conditions for the lighter generations do not hold, though, in our data sample.

Besides case A, where only the channel $\widehat{\delta\phi} \rightarrow N_1^c N_1^c$ is kinematically unblocked, $\widehat{\delta\phi}$ decays into N_1^c 's and N_2^c 's. In the latter cases ε_2 yields the dominant contribution to the calculation Y_B from Eq. (87). From our computation, we also

TABLE VI: Parameters yielding the correct BAU for $K = K_2$ or K_3 , $n = 0.02$, $\lambda_\mu = 10^{-6}$, $y_3 = 0.5$ and various neutrino mass schemes.

PARAMETERS	CASES						
	A	B	C	D	E	F	G
	Normal Hierarchy		Almost Degeneracy			Inverted Hierarchy	
Low Scale Parameters (Masses in eV)							
$m_{1\nu}/0.1$	0.01	0.1	0.5	0.7	0.7	0.5	0.49
$m_{2\nu}/0.1$	0.09	0.13	0.51	1.0	0.705	0.51	0.5
$m_{3\nu}/0.1$	0.5	0.51	0.71	1.12	0.5	0.1	0.05
$\sum_i m_{i\nu}/0.1$	0.6	0.74	1.7	2.3	1.9	1.1	1
$m_\beta/0.01$	0.22	0.98	3.5	5.3	2.9	4.9	3.6
φ_1	0	0	0	$\pi/2$	$\pi/2$	$-3\pi/4$	0
φ_2	$-\pi/2$	0	$\pi/2$	$-\pi$	$-2\pi/3$	$5\pi/4$	$-\pi/2$
Leptogenesis-Scale Mass Parameters in GeV							
m_{1D}	1.98	1.5	2.3	4.16	5.2	1	6.3
m_{2D}	38	16.6	12	10	9.6	6.6	10
$m_{3D}/100$	1	1	1	1	1	1	0.33
$M_{1N^c}/10^{11}$	1.6	2.1	1.4	2.8	5.2	0.2	8.9
$M_{2N^c}/10^{12}$	27	6.8	2.6	4.8	1.9	2.2	3.2
$M_{3N^c}/10^{14}$	22	4.7	0.89	0.22	0.69	2.9	0.9
Decay channels of the Inflaton $\widehat{\delta\phi}$							
$\widehat{\delta\phi} \rightarrow$	N_1^c	$N_{1,2}^c$	$N_{1,2}^c$	$N_{1,2}^c$	$N_{1,2}^c$	$N_{1,2}^c$	$N_{1,2}^c$
Resulting B -Yield							
$Y_B^0/10^{-11}$	9.63	8	8.4	9.1	8.9	8.7	8.9
$Y_B/10^{-11}$	8.67	8.59	8.69	8.56	8.65	8.67	8.65
Resulting T_{rh} (in GeV) and \widetilde{G} -Yield							
$T_{\text{rh}}/10^9$	1	1.1	1	1.1	1	1	1
$10^{13} Y_{3/2}$	1.91	2.2	1.9	2	1.9	1.9	1.97

remark that $\widehat{\Gamma}_{\delta\phi \rightarrow N_i^c N_i^c} < \widehat{\Gamma}_{\delta\phi \rightarrow H_u H_d} < \widehat{\Gamma}_{\delta\phi \rightarrow XYZ}$, and so the ratios $\widehat{\Gamma}_{\delta\phi \rightarrow N_i^c N_i^c} / \widehat{\Gamma}_{\delta\phi}$ introduce a considerable reduction (0.02 – 0.25) in the derivation of Y_B . As a consequence, the attainment of the correct Y_B requires relatively large m_{iD} 's with $i = 1, 2$ in order to achieve sizable enough $\widehat{\Gamma}_{\delta\phi \rightarrow N_i^c N_i^c}$. Namely, $m_{1D} \gtrsim 1$ GeV and $m_{2D} \gtrsim 6.6$ GeV. Besides case A, the first inequality is necessary, in order to fulfill the second inequality in Eq. (89), given that m_{1D} heavily influences M_{1N^c} . In Table VII we list only m_{1D} in case A or m_{2D} in the other cases which are adjusted so as to accommodate Y_B within the range of Eq. (88) with the others m_{iD} remaining as shown in Table VI. As a consequence, M_{iN^c} deviate very little from the values shown in Table VI.

In both Tables we also display, for comparison, the B -yield with (Y_B) or without (Y_B^0) taking into account the renormalization group effects. We observe that the two results are mostly close to each other. Shown also are values for T_{rh} , the

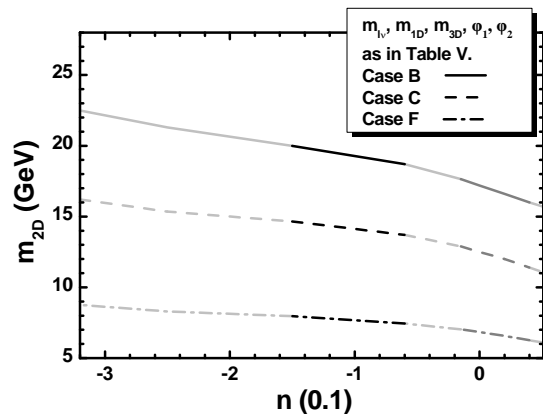
TABLE VII: Same as in Table VI but for $K = K_{2\mathcal{R}}$ and $n = 0$.

PARAMETERS	CASES						
	A	B	C	D	E	F	G
Low Scale Parameters as in Table VI							
Leptogenesis-Scale Mass Parameters in GeV							
$m_{iD}^{(*)}$	1.91	16.6	11.6	10.15	9.25	6.37	9.5
(*) Where $i = 1$ for case A and $i = 2$ for the others.							
The remaining m_{iD} and M_{iN^c} are as in Table VI.							
Resulting B -Yield							
$Y_B^0/10^{-11}$	9.6	7.8	8.5	8.9	8.9	8.9	8.7
$Y_B/10^{-11}$	8.64	8.61	8.72	8.6	8.73	8.8	8.5
Resulting T_{rh} (in GeV) and \tilde{G} -Yield							
$T_{\text{rh}}/10^8$	7.6	8.4	7.7	8.4	7.6	7.6	7.8
$Y_{3/2}/10^{-13}$	1.44	2.9	1.5	1.6	1.45	1.45	1.5

majority of which are close to 10^9 GeV, and the corresponding $Y_{3/2}$'s, with the results for $K = K_{2\mathcal{R}}$ being a little lower. Thanks to our non-thermal set-up, successful leptogenesis can be accommodated with T_{rh} 's lower than those necessitated in the thermal regime – cf. Ref. [66]. The resulting large $Y_{3/2}$'s may be consistent with Eq. (92) mostly for $m_{3/2} \gtrsim 10$ TeV. These are marginally tolerated with the $m_{3/2}$'s appearing in Table V and Figs. 2 and 3 of Ref. [58] in the A/H funnel and $\chi_1^\pm - \chi$ coannihilation regions – see also Ref. [67]. These $m_{3/2}$'s though are more easily reconciled with low energy data in less restrictive versions of MSSM – see e.g. Ref. [68].

In order to extend the conclusions inferred from Table VI to the case of variable n , we can examine how the central value of Y_B in Eq. (88) can be achieved by varying m_{2D} as a function of n . The resulting contours in the $n - m_{2D}$ plane are presented in Fig. 6 – since the range of Y_B in Eq. (88) is very narrow, the 95% c.l. width of these contours is negligible. The convention adopted for these lines is also described in the figure. In particular, we use solid, dashed, or dot-dashed line for m_{iD} , m_{1D} , m_{3D} , φ_1 , and φ_2 corresponding to the cases B, D, or F of Table VI respectively. For n within its allowed margins in Eqs. (65) and (66) we obtain $0.4 \lesssim T_{\text{rh}}/10^9$ GeV $\lesssim 1.8$, which is perfectly acceptable from Eq. (92) for $m_{3/2} \gtrsim 10$ TeV. Along the depicted contours, the resulting M_{2N^c} 's vary in the ranges $(5.7 - 14.5) \cdot 10^{12}$ GeV, $(1.8 - 4.6) \cdot 10^{12}$ GeV, $(1.5 - 3.9) \cdot 10^{12}$ GeV for cases B, C and F respectively, whereas M_{1N^c} and M_{3N^c} remain close to their values presented in the corresponding cases of Table VI.

Comparing, finally, our results above with those presented in Ref. [23], we can deduce that here $\hat{m}_{\delta\phi}$ and T_{rh} gain almost their maximal allowed values since r_\pm is also maximized due to the hypothesis of Eq. (38). As a consequence, $m_{3/2}$ also has to be enhanced to avoid problems with BBN, whereas $m_{1,2D}$ and $M_{1,2N^c}$ are also constrained to larger values. On the other hand, our results are closer to those obtained employing the model of IG in Ref. [3] with gauge singlet inflaton and without unification constraint.

**FIG. 6:** Contours in the $n - m_{2D}$ plane yielding the central Y_B in Eq. (88) consistently with the inflationary requirements for $K = K_2$ or K_3 , $\lambda_\mu = 10^{-6}$, $y_3 = 0.5$ and the values of m_{iD} , m_{1D} , m_{3D} , φ_1 , and φ_2 which correspond to the cases B (solid line), C (dashed line), and F (dot-dashed line) of Table VI. The color coding is as in Fig. 3.

IV. CONCLUSIONS

We have proposed a class of novel inflationary models, in which a Higgs field plays the role of the inflaton, before settling in its final vacuum state where it generates the Planck scale and gives rise to a mass for the gauge boson consistent with gauge coupling unification within MSSM. These two hypotheses allow us to determine the mass scale M , entering W_{HI} in Eq. (1), and $c_{\mathcal{R}}$ for the K 's in Eqs. (4a) and (4b) or $r_\pm = c_+/c_-$ for the K 's in Eqs. (6a) – (6c). In the latter cases, r_\pm expresses the amount of violation of a shift symmetry. As a consequence, the inflationary scenario depends essentially on two free parameters – n and λ or λ/c_- for the first or second group of K 's, respectively – leading naturally to observationally acceptable results. Namely, for the K 's in Eqs. (6a) – (6c) we obtained slightly larger r 's and two distinct allowed regions of parameters with n values one order of magnitude larger than those needed for the K 's in Eqs. (4a) and (4b). As an example, the model for $K = K_2$ or K_3 , $n = 0$ and $\lambda/c_- = 3 \cdot 10^{-5}$ yields $n_s \simeq 0.973$ and $r \simeq 0.0066$ with negligibly small a_s . In all cases, inflation is attained for subplanckian inflaton values, thereby stabilizing our predictions from possible higher order corrections, whereas the corresponding effective theories remain trustable up to m_{P} .

The models were further extended to generate the MSSM μ parameter, consistently with the low energy phenomenology. Successful baryogenesis is achieved via primordial leptogenesis, in agreement with the data on neutrino masses and mixing. More specifically, our post-inflationary setting favors the A/H funnel and the $\tilde{\chi}_1^\pm - \chi$ coannihilation regions of CMSSM with gravitino heavier than about 10 TeV. Leptogenesis is realized through the out-of-equilibrium decay of the inflaton to the right-handed neutrinos N_1^c and/or N_2^c , with masses lower than $3.5 \cdot 10^{13}$ GeV, and reheat temperature T_{rh} close to 10^9 GeV.

ACKNOWLEDGMENTS

C.P. acknowledges the Bartol Research Institute and the Department of Physics and Astronomy of the University of

Delaware for its warm hospitality, during which this work has been initiated. He also acknowledges useful discussions with G. Lazarides and S. Martin. Q.S. acknowledges support by the DOE grant No. DE-SC0013880.

REFERENCES

- [1] A. Zee, *Phys. Rev. Lett.* **42**, 417 (1979); H. Terazawa, *Phys. Lett. B* **101**, 43 (1981).
- [2] A.A. Starobinsky, *Phys. Lett. B* **91**, 99 (1980).
- [3] C. Pallis, *J. Cosmol. Astropart. Phys.* **04**, 024 (2014); **07**, 01(E) (2017) [arXiv:1312.3623].
- [4] R. Kallosh, *Phys. Rev. D* **89**, 087703 (2014) [arXiv:1402.3286].
- [5] C. Pallis, *J. Cosmol. Astropart. Phys.* **08**, 057 (2014) [arXiv:1403.5486]; C. Pallis, *J. Cosmol. Astropart. Phys.* **10**, 058 (2014) [arXiv:1407.8522]; C. Pallis, *PoS CORFU 2014*, 156 (2015) [arXiv:1506.03731].
- [6] C. Pallis and N. Toumbas, *J. Cosmol. Astropart. Phys.* **05**, no. 05, 015 (2016) [arXiv:1512.05657]; C. Pallis and N. Toumbas, *Adv. High Energy Phys.* **2017**, 6759267 (2017) [arXiv:1612.09202]; C. Pallis, *PoS EPS-HEP 2017*, 047 (2017) [arXiv:1710.04641].
- [7] M.B. Einhorn and D.R.T. Jones, *J. Cosmol. Astropart. Phys.* **11**, 049 (2012) [arXiv:1207.1710].
- [8] F.S. Accetta, D.J. Zoller, and M.S. Turner, *Phys. Rev. D* **31**, 3046 (1985); R. Fakir and W.G. Unruh, *Phys. Rev. D* **41**, 1792 (1990); D.I. Kaiser, *Phys. Rev. D* **52**, 4295 (1995) [astro-ph/9408044].
- [9] D.S. Salopek, J.R. Bond and J.M. Bardeen, *Phys. Rev. D* **40**, 1753 (1989); J.L. Cervantes-Cota and H. Dehnen, *Phys. Rev. D* **51**, 395 (1995) [astro-ph/9412032].
- [10] N. Kaloper, L. Sorbo and J. Yokoyama, *Phys. Rev. D* **78**, 043527 (2008) [arXiv:0803.3809].
- [11] G.F. Giudice and H.M. Lee, *Phys. Lett. B* **733**, 58 (2014) [arXiv:1402.2129].
- [12] K. Kannike *et al.*, *J. High Energy Phys.* **05**, 065 (2015) [arXiv:1502.01334]; M.B. Einhorn and D.R.T. Jones, *J. High Energy Phys.* **01**, 019 (2016) [arXiv:1511.01481].
- [13] P.A.R. Ade *et al.* [Planck Collaboration], *Astron. Astrophys.* **594**, A20 (2016) [arXiv:1502.02114].
- [14] J.L.F. Barbon and J.R. Espinosa, *Phys. Rev. D* **79**, 081302 (2009) [arXiv:0903.0355]; C.P. Burgess, H.M. Lee and M. Trott, *J. High Energy Phys.* **07**, 007 (2010) [arXiv:1002.2730].
- [15] A. Kehagias, A.M. Dizgah and A. Riotto, *Phys. Rev. D* **89**, 043527 (2014) [arXiv:1312.1155].
- [16] C. Pallis, *Phys. Lett. B* **692**, 287 (2010) [arXiv:1002.4765].
- [17] R. Kallosh, A. Linde and D. Roest, *Phys. Rev. Lett.* **112**, 011303 (2014) [arXiv:1310.3950].
- [18] N. Okada, M.U. Rehman, and Q. Shafi, *Phys. Rev. D* **82**, 043502 (2010) [arXiv:1005.5161].
- [19] C. Pallis and N. Toumbas, *J. Cosmol. Astropart. Phys.* **12**, 002 (2011) [arXiv:1108.1771]; C. Pallis and N. Toumbas, "Open Questions in Cosmology" (InTech, 2012) [arXiv:1207.3730].
- [20] G. Lazarides and C. Pallis, *J. High Energy Phys.* **11**, 114 (2015) [arXiv:1508.06682].
- [21] C. Pallis, *Phys. Rev. D* **92**, no. 12, 121305(R) (2015) [arXiv:1511.01456].
- [22] C. Pallis, *J. Cosmol. Astropart. Phys.* **10**, no. 10, 037 (2016) [arXiv:1606.09607].
- [23] C. Pallis, *Universe* **4**, no. 1, 13 (2018) [arXiv:1510.05759].
- [24] G.R. Dvali, Q. Shafi and R.K. Schaefer, *Phys. Rev. Lett.* **73**, 1886 (1994) [hep-ph/9406319].
- [25] G.R. Dvali, G. Lazarides and Q. Shafi, *Phys. Lett. B* **424**, 259 (1998) [hep-ph/9710314].
- [26] M. Bastero-Gil, S.F. King and Q. Shafi, *Phys. Lett. B* **651**, 345 (2007) [hep-ph/0604198]; B. Garbrecht, C. Pallis and A. Pilaftsis, *J. High Energy Phys.* **12**, 038 (2006) [hep-ph/0605264]; M.U. Rehman, V.N. Şenoğuz and Q. Shafi, *Phys. Rev. D* **75**, 043522 (2007) [hep-ph/0612023]; C. Pallis, *J. Cosmol. Astropart. Phys.* **04**, 024 (2009) [arXiv:0902.0334]; M. Civeletti, C. Pallis and Q. Shafi, *Phys. Lett. B* **733**, 276 (2014) [arXiv:1402.6254].
- [27] V.N. Şenoğuz and Q. Shafi, hep-ph/0512170; W. Buchmüller, V. Domcke and K. Schmitz, *Nucl. Phys.* **B862**, 587 (2012) [arXiv:1202.6679]; C. Pallis and Q. Shafi, *Phys. Lett. B* **725**, 327 (2013) [arXiv:1304.5202].
- [28] N. Okada and Q. Shafi, *Phys. Lett. B* **775**, 348 (2017) [arXiv:1506.01410].
- [29] N. Okada and Q. Shafi, arXiv:1709.04610.
- [30] M. Kawasaki, M. Yamaguchi and T. Yanagida, *Phys. Rev. Lett.* **85**, 3572 (2000) [hep-ph/0004243]; P. Brax and J. Martin, *Phys. Rev. D* **72**, 023518 (2005) [hep-th/0504168]; S. Antusch, K. Dutta and P.M. Kostka, *Phys. Lett. B* **677**, 221 (2009) [arXiv:0902.2934]; R. Kallosh, A. Linde and T. Rube, *Phys. Rev. D* **83**, 043507 (2011) [arXiv:1011.5945]; T. Li, Z. Li and D.V. Nanopoulos, *J. Cosmol. Astropart. Phys.* **02**, 028 (2014) [arXiv:1311.6770]; K. Harigaya and T.T. Yanagida, *Phys. Lett. B* **734**, 13 (2014) [arXiv:1403.4729]; A. Mazumdar, T. Noumi and M. Yamaguchi, *Phys. Rev. D* **90**, 043519 (2014) [arXiv:1405.3959]; C. Pallis and Q. Shafi, *Phys. Lett. B* **736**, 261 (2014) [arXiv:1405.7645].
- [31] I. Ben-Dayan and M.B. Einhorn, *J. Cosmol. Astropart. Phys.* **12**, 002 (2010) [arXiv:1009.2276].
- [32] C. Pallis, *Phys. Rev. D* **91**, no. 12, 123508 (2015) [arXiv:1503.05887]; C. Pallis, *PoS PLANCK 2015*, 095 (2015) [arXiv:1510.02306].
- [33] P.A.R. Ade *et al.* [BICEP2/Keck Array Collaborations], *Phys. Rev. Lett.* **116**, 031302 (2016) [arXiv:1510.09217].
- [34] W.L.K. Wu *et al.*, *J. Low. Temp. Phys.* **184**, no. 3-4, 765 (2016) [arXiv:1601.00125].
- [35] P. Andre *et al.* [PRISM Collaboration], arXiv:1306.2259.
- [36] T. Matsumura *et al.*, *J. Low. Temp. Phys.* **176**, 733 (2014) [arXiv:1311.2847].
- [37] F. Finelli *et al.* [CORE Collaboration] arXiv:1612.08270.
- [38] K. Hamaguchi, *Phd Thesis* [hep-ph/0212305]; W. Buchmüller, R.D. Peccei and T. Yanagida, *Ann. Rev. Nucl. Part. Sci.* **55**, 311 (2005) [hep-ph/0502169].
- [39] G. Lazarides and Q. Shafi, *Phys. Lett. B* **258**, 305 (1991); K. Kumekawa, T. Moroi and T. Yanagida, *Prog. Theor. Phys.* **92**, 437 (1994) [hep-ph/9405337]; G. Lazarides, R.K. Schaefer and Q. Shafi, *Phys. Rev. D* **56**, 1324 (1997)

- [hep-ph/9608256]; V.N. Şenoğuz and Q. Shafi, *Phys. Rev. D* **71**, 043514 (2005) [hep-ph/0412102].
- [40] M.Yu. Khlopov and A.D. Linde, *Phys. Lett. B* **138**, 265 (1984); J. Ellis, J.E. Kim, and D.V. Nanopoulos, *Phys. Lett. B* **145**, 181 (1984).
- [41] M. Bolz, A.Brandenburg and W. Buchmüller, *Nucl. Phys.* **B606**, 518 (2001); **790**, 336(E) (2008) [hep-ph/0012052]; J. Pradler and F.D. Steffen, *Phys. Rev. D* **75**, 023509 (2007) [hep-ph/0608344].
- [42] M.Kawasaki, K.Kohri and T.Moroi, *Phys. Lett. B* **625**, 7 (2005) [astro-ph/0402490]; M. Kawasaki, K. Kohri and T. Moroi, *Phys. Rev. D* **71**, 083502 (2005) [astro-ph/0408426]; J.R. Ellis, K.A. Olive and E. Vangioni, *Phys. Lett. B* **619**, 30 (2005) [astro-ph/0503023]; M. Kawasaki, K. Kohri, T. Moroi and Y. Takaesu, *Phys. Rev. D* **97**, no. 2, 023502 (2018) [arXiv:1709.01211].
- [43] J. Ellis *et al.*, *J. Cosmol. Astropart. Phys.* **03**, no. 03, 008 (2016) [arXiv:1512.05701]; Y. Ema *et al.*, *J. High Energy Phys.* **11**, 184 (2016) [arXiv:1609.04716].
- [44] D.V. Forero, M. Tortola and J.W.F. Valle, *Phys. Rev. D* **90**, no. 9, 093006 (2014) [arXiv:1405.7540].
- [45] M.C. Gonzalez-Garcia, M. Maltoni and T. Schwetz, *J. High Energy Phys.* **11**, 052 (2014) [arXiv:1409.5439]; F. Capozzi *et al.*, *Nucl. Phys. B* **908**, 218 (2016) [arXiv:1601.07777].
- [46] M.B. Einhorn and D.R.T. Jones, *J. High Energy Phys.* **03**, 026 (2010) [arXiv:0912.2718]; H.M. Lee, *J. Cosmol. Astropart. Phys.* **08**, 003 (2010) [arXiv:1005.2735]; S. Ferrara *et al.*, *Phys. Rev. D* **83**, 025008 (2011) [arXiv:1008.2942]; C. Pallis and N. Toumbas, *J. Cosmol. Astropart. Phys.* **02**, 019 (2011) [arXiv:1101.0325].
- [47] G. Lopes Cardoso, D. Lüst and T. Mohaupt, *Nucl. Phys.* **B432** 68 (1994) [hep-th/9405002]; I. Antoniadis, E. Gava, K.S. Narain and T.R. Taylor, *Nucl. Phys.* **B432** 187 (1994) [hep-th/9405024].
- [48] R. Kallosh, A. Linde and D. Roest, *J. High Energy Phys.* **11**, 198 (2013) [arXiv:1311.0472]; R. Kallosh, A. Linde and D. Roest, *J. High Energy Phys.* **08**, 052 (2014) [arXiv:1405.3646].
- [49] L. Boubekeur and D. Lyth, *J. Cosmol. Astropart. Phys.* **07**, 010 (2005) [hep-ph/0502047].
- [50] S.R. Coleman and E.J. Weinberg, *Phys. Rev. D* **7**, 1888 (1973).
- [51] D.H. Lyth and A. Riotto, *Phys. Rept.* **314**, 1 (1999) [hep-ph/9807278]; J. Martin, C. Ringeval and V. Vennin, *Physics of the Dark Universe* **5-6**, 75 (2014) [arXiv:1303.3787].
- [52] <http://functions.wolfram.com>.
- [53] P.A.R. Ade *et al.* [Planck Collaboration], *Astron. Astrophys.* **594**, A13 (2016) [arXiv:1502.01589].
- [54] A. Racioppi, arXiv:1801.08810.
- [55] G. Lazarides and Q. Shafi, *Phys. Rev. D* **58**, 071702 (1998) [hep-ph/9803397].
- [56] S. Antusch and M. Spinrath, *Phys. Rev. D* **78**, 075020 (2008) [arXiv:0804.0717].
- [57] W. Buchmüller *et al.*, *J. High Energy Phys.* **09**, 053 (2014) [arXiv:1407.0253]; J. Ellis, M. Garcia, D. Nanopoulos and K. Olive, *J. Cosmol. Astropart. Phys.* **10**, 003 (2015) [arXiv:1503.08867]; E. Dudas, T. Gherghetta, Y. Mambrini and K.A. Olive, *Phys. Rev. D* **96**, no. 11, 115032 (2017) [arXiv:1710.07341].
- [58] P. Athron *et al.* [GAMBIT Collaboration], *Eur. Phys. J. C* **77**, no. 12, 824 (2017) [arXiv:1705.07935].
- [59] A. Addazi, S.V. Ketov and M.Y. Khlopov, arXiv:1708.05393.
- [60] M. Endo, F. Takahashi and T.T. Yanagida, *Phys. Rev. D* **76**, 083509 (2007) [arXiv:0706.0986].
- [61] C. Pallis, *Nucl. Phys.* **B751**, 129 (2006) [hep-ph/0510234].
- [62] S.V. Ketov and A.A. Starobinsky, *Phys. Rev. D* **83**, 063512 (2011) [arXiv:1011.0240]; S. V. Ketov and N. Watanabe, *J. Cosmol. Astropart. Phys.* **03**, 011 (2011) [arXiv:1101.0450]; S.V. Ketov and A.A. Starobinsky, *J. Cosmol. Astropart. Phys.* **08**, 022 (2012) [arXiv:1203.0805]; S.V. Ketov and S. Tsujikawa, *Phys. Rev. D* **86**, 023529 (2012) [arXiv:1205.2918].
- [63] S. Antusch, J. Kersten, M. Lindner and M. Ratz, *Nucl. Phys.* **B674**, 401 (2003) [hep-ph/0305273].
- [64] V.N. Şenoğuz, *Phys. Rev. D* **76**, 013005 (2007) [arXiv:0704.3048].
- [65] A. Gando *et al.* [KamLAND-Zen Collaboration], *Phys. Rev. Lett* **117**, no.8, 082503.(2016); *ibid* **17**, no.10, 109903 (2016) [arXiv:1605.02889].
- [66] S. Antusch and A.M. Teixeira, *J. Cosmol. Astropart. Phys.* **02**, 024 (2007) [hep-ph/0611232].
- [67] N. Karagiannakis, G. Lazarides and C. Pallis, *Phys. Rev. D* **92**, no. 8, 085018 (2015) [arXiv:1503.06186].
- [68] H. Baer *et al.*, *Phys. Rev. Lett.* **109**, 161802 (2012) [arXiv:1207.3343].